Final Report

Modeling of Zero Gravity Venting

by

Herman Merte, Jr.

GRANT NAG 3 403

Studies of Two-Phase Heat Transfer
Under Reduced Gravity

NATIONAL AERONAUTICS
AND SPACE ADMINISTRATION
NASA/Lewis Research Center

College of Engineering

Department of Mechanical Engineering & Applied Mechanics

The University of Michigan

Ann Arbor, Michigan 48109

020547-FR

Final Report

Modeling of Zero Gravity Venting

by

Herman Merte, Jr.

GRANT NAG 3 403

Studies of Two-Phase Heat Transfer
Under Reduced Gravity

NATIONAL AERONAUTICS
AND SPACE ADMINISTRATION
NASA/Lewis Research Center

THE UNIVERSITY OF MICHIGAN

COLLEGE OF ENGINEERING

Department of Mechanical Engineering and Applied Mechanics

Heat Transfer Laboratory

Administered Through:

DIVISION OF RESEARCH DEVELOPMENT AND ADMINISTRATION

ANN ARBOR, MICHIGAN

August 1986

TABLE OF CONTENTS

ABSTRACT

The objective of this study is to predict the pressure response of a saturated liquid-vapor system when undergoing a venting or depressurization process in zero gravity at low vent rates. An experimental investigation of the venting of cylindrical containers partially filled with initially saturated liquids was previously conducted under zero-gravity conditions at the NASA Lewis Research Center 5-second zero gravity facility, and compared with an analytical model which incorporated the effect of interfacial mass transfer on the ullage pressure response during venting. A new model is presented here to improve the estimation of the interfacial mass transfer. Duhammel's superposition integral is incorporated to approximate the transient temperature response of the interface, treating the liquid as a semi-infinite solid with conduction heat transfer. Account is also taken of the condensation taking place within the bulk of a saturated vapor as isentropic expansion takes place. Computational results are presented for the venting of R-11 from a given vessel and initial state for five different venting rates over a period of three seconds, and are compared to the prior NASA experiments. An improvement in the prediction of the final pressure takes place, but is still considerably below the measurements. This is attributed to neglecting the evaporation taking place at the meniscus.

I. INTRODUCTION

This is a report of an analytic study of the venting process, under microgravity, of a container with liquid-vapor phases. Pure substances only are considered here. It may be desireable to extend the analysis later to mixtures of substances having different boiling points should the possibility arise for the future storage of such mixtures in space.

Microgravity indicates the drastic reduction of body forces which, in turn, implies the drastic reduction of natural convection motion associated with temperature differences within the fluid(s). With liquid-vapor phases present, this also implies that effects associated with surface tension may become significant. These effects include the absence of a flat interface, the possible presence of thermophorysis, and the variable location of the vapor volume. This latter is important for the venting process in practice, since the process desired must be specified, whether venting of pure vapor, pure liquid, or a mixture of both. For purposes of the present study surface tension is considered only insofar as it affects the amount of liquid-vapor interfacial area and the contact angle made at the solid-liquid-vapor contact region. The curvature may be neglected in the description of the temperature distribution in the liquid near the liquid-vapor interface, except where very small vapor bubbles are present. Such would mean that vapor nucleation and boiling are taking place, which are also excluded from consideration at present.

The objective of the study is to model the venting process so as to be able to predict the pressure-time behavior within the

container, incorporating the relevent physical mechanisms. In the broadest sense the process is similar to the problem of describing the blowdown taking place in a nuclear power plant loss-of-coolant accident (LOCA). Because of its importance to the safety of nuclear power plants many studies of this have been conducted, and an abundance of literature exists. However, very little is directly applicable to the present problem.

The LOCA is generally an uncontrolled process in that the circumstance as to the location and size of the discharge opening is not known in advance. The fluid discharged may be liquid only, vapor only, or a mixture of the two, depending on the location and size of the opening. If the opening is sufficiently small the pressure decrease may be described reasonably well by assuming saturation properties within the vessel, provided the two-phase critical flow occuring at the opening is properly modelled. Some difficulties still exist in achieving this [1,2] without introducing some degree of empiricism for the discharge coefficient. If the opening is relatively large the pressure drops so rapidly that bulk vapor nucleation occurs with a two-phase discharge. The upper limit of this is the pipe blowdown problem: A one-dimensional analysis and confirming experiments of this process, beginning with a subcooled liquid, were conducted [3] in which the time for complete discharge was on the order of 200-300 ms.

The zero gravity venting problem under consideration here, on the other hand, is expected to be a more orderly and planned process. Nevertheless, the description of the physical process can become relatively complex when the transient behavior in the

vicinity of the liquid-vapor interface is taken into consideration. An analysis of the adiabatic venting of the homogeneous two-phase contents of a vessel was conducted, assuming equilibrium saturation conditions [4]. A special model for choked two-phase flow at the discharge opening was derived and used. Since equilibrium conditions were assumed, the size and location of the vapor during the process was irrelevent. In a later work [5], the same author attempted to include vapor generation associated with external heat transfer in the process, retaining the assumption of internal thermodynamic equilibrium. In addition, various venting locations were considered: Vapor venting only (top vapor blowdown), liquid venting only (bottom liquid blowdown), and bottom mixture blowdown.

The zero gravity venting problem at hand is concerned only with the venting of vapor, either with a known vent rate or vent size. It is further considered that the venting rate is sufficiently slow that no vapor nucleating sites are formed, so that any phase changes taking place occur only at existing interfaces. This places an upper limit on the rate of pressure drop permissible [6,7,8].

It has been demonstrated that models assuming thermodynamic equilibrium can give reasonable results only with the inclusion of sufficient empirical coefficients, since non-equilibrium conditions in fact are present. The challenge is to minimize the number of empirical coefficients, using non-equilibrium analysis only for those aspects of the process where it has a significant role.

The work reported below is an extension of the analysis presented in [9], employing a different model for the estimation of the mass transfer at the liquid-vapor interface and in including the phase change associated with the expansion of the saturated vapor as the venting process takes place. Discrepancies still exist between the computations conducted here and the experimental results reported in [9], with the model predicting a greater pressure decrease than is measured. The transient temperature at the liquid-vapor interface is computed by incorporating Duhammel's superposition integral in the analysis, treating the liquid as a one-dimensional semi-infinite solid with conduction heat transfer. It is believed that evaporation taking place at the meniscus at the liquid-vapor-wall interline, neglected in all analyses to date, can play a significant role relative to that occuring at the bulk liquid interface [10].

II. ANALYSIS

A schematic of the venting system is shown in Figure 1. The venting of vapor only is considered here. It is assumed the $P_v(t)$ is sufficiently greater than P_∞ at all times so the venting rate itself can be described reasonably well in terms of choked flow, assuming that only single phase flow occurs and that an appropriate flow coefficient can be assigned. It is further assumed that all the heat transfer processes of significance are one-dimensional, whether at the interfacial area A_i in Figure 1 or at the meniscus L_m in Figure 2. At the present time these are the only domains in which heat transfer and phase changes will be

considered to take place. The effect of microgravity relative to other gravities is presumed to change only the absolute and relative magnitudes of the interfacial area A_i and meniscus length L_m. The processes occuring in the vapor space due to the pressure decrease with venting will be considered first.

1. Vapor Region

As the pressure decreases, the initially saturated vapor at state (1) remaining in the container can be presumed to have undergone a reversible adiabatic expansion. This ignores, for the moment, any interaction with vapor which might be generated at the liquid-vapor interface. Referring to Figure 3, it can be noted that if local equilibrium exists during the process the state will be at (2), a temperature decrease will have taken place, and liquid must have formed within the vapor to produce the quality required by the state. Since the liquid interface and any vapor generated at the interface would be at the instantaneous saturation temperature corresponding to the system prssure, with equilibrium no temperature gradients would exist within the vapor space, nor need they be considered; the temperature and pressure within the vapor space are coupled. However, the presence of quality in the vapor space introduces two aspects in the problem not considered heretofore: The quality itself must now be included within the state description of the vapor, and homogeneous bulk nucleation must take place within the vapor space to produce the uniform quality assumed. Homogeneous bulk nucleation requires that the vapor itself be subcooled to some degree [11]. The container walls could provide

nucleation sites, requiring an amount of subcooling so small as to be negligible. One limit then is to neglect the conditions necessary for nucleation, assuming that thermodynamic equilibrium exists in the vapor space at all times.

If no nucleation sites were available, either in the vapor bulk or on the walls, for an expansion to pressure P_2 the vapor will follow the isentropic process to the metastable state (2M) in Figure 3. This is at a lower temperature than the equilibrium state (2) because no latent heat associated with phase change was given up. For this case, the liquid-vapor interface would be at temperature T_2, the T_{sat} corresponding to P_2, while the bulk vapor would be at T_{2M}. A temperature gradient thus would exist within the vapor space, which must then be taken into consideration because of the associated heat transfer. The other limit to that cited above, which still takes the vapor to be at a uniform state, is to consider that the vapor itself exists in a metastable state, with no heat transfer interaction with the interface, but that instantaneous perfect mixing takes place with the vapor produced at the liquid-vapor interface. The resulting mixture would itself be at a metastable state.

To compare the effects of treating the expansion of a saturated vapor with equilibrium into the quality region with that assuming that no condensation occurs, considering that the vapor remains a pure vapor in metastable equilibrium (termed a pseudo-vapor here), sample computations will be presented below for the isentropic expansion of the contents of a tank initially containing only vapor. Certain assumptions will be made for convenience

here, to be eliminated when returning to the original venting problem.

Assumptions:

i. The initial contents of the tank is saturated vapor only.

ii. The contents remaining in the tank at any point will be considered to have a uniform state and to have expanded reversibly and adiabatically. For computation purposes here, the tank will be vented until one-half of the original mass remains.

iii. The expansion of the tank's contents will be treated as a non-rate process. With a uniform state assumed within the tank, the state of the contents is independent of the rate of venting.

In Figure 3, the initial saturated vapor state is designated as (1), and the final specific volume will be $v_2 = 2v_1$ with one-half of the original mass vented. State (2) on the T-S diagram is the isentropic end state in the equilibrium quality region, while state (2P) is the isentropic end state with pseudo-vapor behavior, with no condensation. Note that $v_2 = v_{2P}$, and the problem is now to compute and compare the corresponding end states P_2, T_2 and P_{2P}, T_{2P}. In general, state (2P) will be different than state (2M), the difference depending on the degree of expansion and on the particular fluid properties. Computations below will demonstrate this.

In both of the above processes, the state of the fluid vented is assumed to have the same property as the bulk property of the fluid in the vessel. For the isentropic expansion in the quality region, the generation of quality requires the formation

of liquid drop nuclei, in the practical sense. These nuclei will form either as a bulk homogeneous nucleation process or a heterogeneous nucleation process taking place on the walls of the container. For the case where bulk liquid is present in the container, such condensation could also occur on the liquid-vapor interface. Since bulk homogeneous nucleation requires a significantly greater degree of supersaturation in the vapor relative to heterogeneous nucleation on the walls, it can be expected that the latter would be much more likely to take place. The implication of this to the venting process is that with the droplet nucleation and condensation now taking place on the walls, the bulk fluid vented would have the state of a saturated vapor only, while the state of the contents of the vessel taken as a whole would have quality. The analysis to determine the end state for a given mass vented would be different from the two cases described above, and would give an end state also different from these.

A brief description of the analysis for each of the three cases mentioned above will be given below, to be followed by the results of sample calculations for R-11 as the working fluid.

Case A - Isentropic Expansion with Equilibrium Quality

Referring to Figure 3, the following conditions apply:

Initial Conditions: T_1, P_1 (P_{sat}) (1)

$$v_1 = v_{g1}$$

Since $m_2 = 1/2 m_1$, it follows that

$$v_2 = 2v_1 = v_{f2} + X_2 v_{fg2} \quad (2)$$

$$S_2 = S_1 = S_{f2} + X_2 S_{fg2} \quad (3)$$

Using tables of thermodynamic properties, $T_2(P_2)$ and X_2 can be determined from Equations (2) and (3).

Case B - Isentropic Expansion as a Pseudo-Vapor

Referring to Figure 3:

Initial conditions: Same as Equation (1) above.

Since it is taken that $m_2 = 1/2m_1$,

$$v_2 = 2v_1 = v_{2S} = v_{2P} \tag{4}$$

The end state 2P is the extension of the constant volume line v_2 into the pseudo-vapor domain such that:

$$S_{2P} = S_1 \tag{5}$$

The entropy change along a constant volume line for low pressure vapor with no phase change is given by:

$$dS = \frac{C_v^o(T)}{T} dT \tag{6}$$

Since state (2S) is known, T_{2P} can be determined from integration of Equation (6) as:

$$S_{2S} - S_{2P} = S_{2S} - S_1 = \int_{T_{2P}}^{T_{2S}} \frac{C_v^o(T)}{T} dT \tag{7}$$

P_{2P} is then computed from v_{2P} and T_{2P} using the appropriate equation of state.

Case C - Isentropic Expansion with Equilibrium Quality and Venting of Saturated Vapor Only

Since the state of the fluid being vented in Cases A and B above is the same as the bulk fluid state, the final result obtained is the same regardless of whether a system or control volume analysis is used. For the case being considered here

where the fluid being vented is a saturated vapor while the bulk fluid remaining in the tank has quality, a control volume analysis must be used.

Initial conditions: Same as Equation (1) above.

As in Cases A and B, it will still be taken that $m_2 = 1/2m_1$. The final state will be designated by the subscript "2V", while the variable intensive properties in the container will have the subscript "σ", and the state of the fluid vented will have the subscript "e".

The control volume form of the first law of thermodynamics for the constant volume insulated container is given by:

$$d(m_\sigma u_\sigma) = -\delta m_e x h_e \tag{8}$$

Expanding the left side, and noting from continuity that $\delta m_e = -dm_\sigma$, and that $h_e = h_{g\sigma}$, Equation (8) can be written as

$$\frac{du_\sigma}{h_{g\sigma} - u_\sigma} = \frac{dm_\sigma}{m_\sigma} \tag{9}$$

Integrating from the initial state "1" to the final state "2V" with $m_{\sigma 2} = 1/2m_{\sigma 1}$,

$$\int_1^{2V} \frac{du_\sigma}{(h_{g\sigma}-u_\sigma)} = \ln \frac{m_{\sigma 2}}{m_{\sigma 1}} = \ln 1/2 = -0.69315 \tag{10}$$

Note that u_σ can be expressed as,

$$u_\sigma = h_f - Pv_f + X(h_{fg}-Pv_{fg}) \tag{11}$$

and $(h_{g\sigma}-u_\sigma)$ as

$$h_{g\sigma} - u_\sigma = h_{fg}(1-X) + Pv_f + XPv_{fg} \tag{12}$$

The quality in equation (12) is an unknown variable at the moment. Since the contents undergo a reversible adiabatic process,

the second law of thermodynamics for the control volume can be written, similar to Equation (8), as:

$$d(m_\sigma S_\sigma) = \delta m_e \times S_e \tag{13}$$

Using continuity $\delta m_e = -dm_\sigma$, and noting that $S_e = S_{g\sigma}$, Equation (13) can be written as:

$$\frac{dS_\sigma}{S_{g\sigma} - S_\sigma} = \frac{dm_\sigma}{m_\sigma} \tag{14}$$

which is similar in form to Equation (9). Note that S_σ can be expressed as

$$S_\sigma = S_f + XS_{fg} \tag{15}$$

and $S_{g\sigma}-S_\sigma$ as

$$S_{g\sigma} - S_\sigma = S_{fg}(1-X) \tag{16}$$

The integrated form of Equation (9) equals the integrated form of Equation (14), and the quality X during the expansion must be determined to satisfy this.

Solutions

Solutions for the venting of an initially saturated vapor from an insulated tank were carried out for Freon-11 for Cases A, B, and C above, using the tabulated thermodynamic properties, the equation of state, and the constant volume specific heat given in Reference [12]. The results are given in Table 1 for two different initial pressures.

For Case C, Equation (10) could be integrated numerically using either the tabulated property values or the equation of state. Case C-1 in Table 1 was obtained by numerical integration of the tabulated properties in [12], while Case C-2 is the result obtained with the equation of state. In both cases it was neces-

sary to determine the unknown quality at each step by trial-and-error in order to satisfy Equation (9).

It may be noted that, although the final pressure for the expansion as a pseudo-vapor (Case B) is just slightly less than that for the expansion in the isentropic quality region (Case A), the final temperature is lower. This is to be anticipated, since the internal energy decrease for the expansion with no phase change must take place more at the expense of the vapor internal energy, with the attendant decrease in temperature.

For the Case C, where only saturated vapor is vented, the final pressure and associated saturation temperature are lower. The final quality is slightly lower than for Case A, reflecting the fact that any condensed vapor is retained within the container.

For the modeling of the original venting problem, where the initial contents of the insulated tank consists of a mixture of saturated liquid and vapor, it appears that Case C above will represent most realistically the process actually taking place. The isentropic expansion of a saturated vapor results in condensation. Condensation nucleation sites must be present for this to occur, and it is highly unlikely that bulk phase homogeneous nucleation will take place with the presence of metal walls unless the tank is very large. However, nucleation and condensation will occur preferentially on the walls and on the existing liquid-vapor interface, maintaining the bulk as saturated vapor, from which the fluid vented is drawn.

The alternative to the equilibrium treatment of the vapor space described here is a non-equilibrium approach, in which

spacewise temperature non-uniformities must be incorporated into the analysis. Before such complexities are introduced, however, it should be demonstrated that such an approach is necessary.

It is the rate model for the tank venting process that is of interest, and before introducing the interaction with the liquid the time element will be incorporated in Case C above, when the tank contains only saturated vapor, initially, and where only the saturated vapor is being vented, the liquid formed due to the condensation occuring as a result of the vapor expansion being retained within the tank.

The continuity equation for the contents of the control volume consisting of the constant volume tank is:

$$\frac{dm_\sigma}{dt} = -\frac{\delta m_e}{dt} \equiv -\dot{m}_e \tag{17}$$

The rate form of the energy equation corresponding to Equation (8) is:

$$\frac{d}{dt}(m_\sigma u_\sigma) = -\dot{m}_e h_e \tag{18}$$

Expanding the left side of Equation (18), substituting Equation (17) and rearranging, noting that only saturated vapor is leaving:

$$m_\sigma \frac{du_\sigma}{dt} = (h_{g\sigma}-u_\sigma)(-\dot{m}_e) \tag{19}$$

The mass flow rate being vented, $\dot{m}_e$, is modeled using a classical choked flow analysis [13]. In the application to the vacuum of space, a choked flow assumption can be expected to be valid, and the exit mass flow rate will be a function of the upstream vapor properties only:

$$\dot{m}_e = \frac{P_V C_D A_i K_D}{(RT_V)^{1/2}} = K_1 \frac{P_V}{T_V^{1/2}} \tag{20}$$

where

$$K_D = \gamma^{1/2}\left[\frac{2}{\gamma + 1}\right]^{\frac{\gamma + 1}{2(\gamma-1)}} \tag{21}$$

and

$$K_1 = \frac{C_D A_i K_D}{R^{1/2}} \tag{22}$$

Solving Equation (19) for dt and substituting for $\dot{m}_e$ from Equation (20):

$$dt = \frac{-m_\sigma}{(h_{g\sigma}-u_\sigma)} \frac{T_V^{1/2}}{K_1 P_V} du_\sigma \tag{23}$$

Equation (23) can be integrated numerically to find the time required to change from the initial state to any other state at a lower pressure. T_v and P_v are related by the vapor pressure curve or the Clausius-Clapyron equation, while the expressions involving u_σ and $h_{g\sigma}$ are given by Equations (11) and (12). m_σ comes from:

$$m_\sigma = V_\sigma / v_\sigma \tag{24}$$

and

$$v_\sigma = v_f + X v_{fg} \tag{25}$$

During the expansion process, the quality X must be solved at each computational step by trial-and-error such that Equation (9) is satisfied at each state along the path. Temperature is used as the computational variable on the right hand side of Equation (23). As will be described later, a number of different sizes and series of temperature steps were investigated.

2. Liquid Region

As the pressure in the vapor domain decreases as a result of the venting process, the temperature at the liquid interface, T_i in Figure 1, will decrease corresponding to the saturation temperature. If the liquid was intially at a uniform temperature this means that a temperature gradient will be established in the liquid, resulting in evaporation at the liquid-vapor interface. As far as the vapor domain control volume is concerned, this represents a vapor mass addition to the vapor space as a saturated vapor corresponding to the system pressure.

The rate form of the continuity equation corresponding to Equation (17) for the vapor space as a control volume is now:

$$\frac{dm_\sigma}{dt} = \dot{m}_i - \dot{m}_e \tag{26}$$

where $\dot{m}_i$ is the mass flow rate of vapor entering the control volume as a result of evaporation at the liquid-vapor interface.

The rate form of the energy equation corresponding to Equation (18) for the vapor space control volume is:

$$\frac{d}{dt}(m_\sigma u_\sigma) = \dot{m}_i h_i - \dot{m}_e h_e \tag{27}$$

Since the vapor entering the vapor space control volume as a result of evaporation is a saturated vapor corresponding to the system pressure, it has the same state as the vapor being vented, designated as $h_{g\sigma}$ in Equation (19). Expanding the left hand side of Equation (27) and rearranging:

$$m_\sigma \frac{du_\sigma}{dt} = (h_{g\sigma}-u_\sigma)(\dot{m}_i-\dot{m}_e) \tag{28}$$

The rate of vapor generation, $\dot{m}_i$, is determined from the conservation of energy equation applied to the liquid-vapor interface. Assuming no heat transfer to the vapor, all energy transferred to the interface by conduction in the liquid results in vaporization of liquid at the interface, given by:

$$q_l = \dot{m}_i h_{fg} \tag{29}$$

For relatively short periods, where the temperature boundary layer is small compared to any radii of curvature present at the interface, the liquid may be treated as a semi-infinite planar solid. The surface area term, A_i, will be that corresponding to the shape the interface takes in zero gravity. The one dimensional form of Fourier's conduction equation for the liquid at the interface is:

$$q_l = -k_l A_i \left(\frac{dT}{dx}\right)\Big|_{x=0} \tag{30}$$

Combining Equations (29) and (30) gives

$$\dot{m}_i = \frac{-k_l A_i \left(\frac{dt}{dx}\right)\Big|_{x=0}}{h_{fg}} \tag{31}$$

The problem of determining the interfacial mass transfer is reduced to determining the temperature gradient of the liquid at the interface, which requires that the transient temperature distribution in the liquid near the l-v interface be determined. If the liquid near the l-v interface can be considered to approximate a one-dimensional semi-infinite solid in it's thermal behavior the analytic solution for a step change in surface temperature, in connection with the finite form of Duhammel's superposition integral, can be used to determine the transient temperature distribution in the liquid. The time varying inter-

face temperature is taken as the saturation temperature corresponding to the instantaneous system pressure, which must be determined appropriately from the system of governing equations.

Accordingly, the differential form of the governing equation and the initial and boundary conditions for the one-dimensional semi-infinite solid, initially at uniform temperature T_o and with a step change in surface temperature to T_i are:

$$\frac{\partial T}{\partial t} = a\frac{\partial^2 T}{\partial x^2} \tag{32}$$

$$T(x,o) = T_o \tag{33}$$

$$T(o,t) = T_i \tag{34}$$

$$T(\infty,t) = T_o \tag{35}$$

The solutions for the temperature distribution and for the temperature gradient are given by [14]:

$$\frac{T(x,t) - T_i}{T_o - T_i} = \text{erf}\left[\frac{x}{2(at)^{1/2}}\right] \tag{36}$$

$$\frac{\partial T}{\partial x}(o,t) = -\frac{T_o - T_i}{(\pi at)^{1/2}} \tag{37}$$

The interface temperature, being the saturation temperature corresponding to the ullage pressure, will be time varying in the present case since the pressure will change as the tank is vented. This time varying boundary condition $T_i(t)$ is incorporated into the solution using Duhammel's superposition integral [14] in the form:

$$\theta(x,t) = \theta_i(o) \cdot \psi(x,t) + \int_o^t \psi(x,t-s)\,\frac{d\theta_i(s)}{ds}\,ds \tag{38}$$

Here,

$$\begin{aligned} \theta(x,t) &= T(x,t) - T_o \\ \theta_i(t) &= T_i(t) - T_o \end{aligned} \tag{39}$$

We let

$$\phi(x,t) \equiv \frac{\theta(x,t)}{\theta_i(t)} \tag{40}$$

$\psi(x,t)$ is the unsteady temperature resulting from a stepwise unit increase in surface temperature, relative to a uniform initial temperature. If the increase is kept at zero until a certain time t-s, and at that instant raised to unity and maintained constant, the new temperature $\phi(x,t)$ may be expressed in terms of $\psi(x,t)$ as

$$\phi(x,t) = \begin{cases} 0 \ , \ t < s \\ \psi(x,t-s) \ , \ t > s \end{cases} \tag{41}$$

The solution for $\psi(x,t)$ is given by Equation (36), transformed to the form of Equation (40) as:

$$\psi(x,t) = \frac{\theta(x,t)}{\theta_i} = \text{erf}\left[\frac{x}{2(at)^{1/2}}\right] \tag{42}$$

Solution of the system of equations for the venting problem would be performed in discrete time steps, and the discrete form of Equation (38) is given by:

$$\theta(x,t) = \theta_i(o) \cdot \psi(x,t) + \sum_{m=1}^{n} \Delta\theta i_m \cdot \psi(x,t-s_m) \tag{43}$$

where

$$\Delta\theta i_m = \theta_i(s_m) - \theta_i(s_{m-1}) \tag{44}$$

Here, n is the total number of time steps into which the process has been divided, m is a running time index, $1<m<n$, and $\Delta\theta i_m$ is the incremental change in surface temperature, related to the system vapor pressure.

Since the temperature gradient at the interface is needed to compute the interfacial mass transfer rate in Equation (31), this can be obtained by differentiating Duhammel's superposition integral Equation (38) as:

$$\frac{\partial\Theta(o,t)}{\partial x} = \theta_i(o)\frac{\partial\Theta}{\partial x}(o,t) + \int_o^t \frac{\partial\psi}{\partial x}(o,t-s)\frac{d\theta_i(s)}{ds}ds \qquad (45)$$

The discrete form of Equation (45) is given by:

$$\frac{\partial\Theta}{\partial x}(o,t) = \theta_i(o)\frac{\partial\psi}{\partial x}(o,t) + \sum_{m=1}^{n}\Delta\Theta_{im} \cdot \frac{\partial\psi}{\partial x}(o,t-s_m) \qquad (46)$$

For a semi-infinite solid with a step increase disturbance:

$$\frac{\partial\psi}{\partial x}(o,t-s_m) = \frac{1}{[\pi a(t-s_m)]^{1/2}} \qquad (47)$$

Substituting Equation (47) into Equation (46), and noting that although for a step initial disturbance that $\partial\psi/\partial x(o,o) = \infty$, $\theta_i(o)$ can be taken as small as desired, so that Equation (46) becomes:

$$\frac{\partial\Theta}{\partial x}(o,t) = \sum_{m=1}^{n}\frac{\Delta\Theta_{im}}{[\pi a(t-s_m)]^{1/2}} \qquad (48)$$

Equation (48) is the form used to compute the interfacial mass transfer rate below. However, another procedure was developed initially to approximate the temperature gradient at the interface and will be described here for the sake of completeness.

The procedure is to compute the instantaneous temperatures at a finite number of points in the liquid near the interface, using Equation (43), and fit these points to a third order polynomial using a least squares fit. The polynomial is of the form:

$$T = A + Bx + Cx^2 + Dx^3 \qquad (49)$$

The temperature gradient of the liquid at the l-v interface, $x = 0$, is then:

$$\left.\frac{dT}{dx}\right|_{x=0} = B \tag{50}$$

The number and spacing of the nodes at which the temperatures of the liquid are to be calculated, and with which the coefficients A, B, C, and D in Equation (49) will be determined, must next be specified. Six nodes were taken arbitrarily as being sufficient to obtain the four coefficients in Equation (49). Intuitively, nodes nearest to the l-v interface will give the most accurate value of the liquid temperature gradient at the l-v interface. The method used was to estimate a temperature penetration depth, δ, taken here to be the depth at which the dimensionless temperature change computed by equation (36) is 95% of the disturbance, or

$$0.95 = \text{erf}\left[\frac{\delta}{2(at)^{1/2}}\right] \tag{51}$$

and

$$\delta = 1.39 \times 2(at)^{1/2} \tag{52}$$

The actual penetration depth would be somewhat less than this value, since the actual system does not undergo a single step change in surface temperature, but rather a transient change in surface temperature. The six equally spaced nodes are taken to be within the 10% of this penetration depth nearest the l-v interface.

Now that the temperature of the liquid at each of the six nodes near the l-v interface is known, the constants A, B, C, and D of Equation (49) may be determined. A least squares algorithm was used [15] which determines the polynomial coefficients which minimize the error between the data points and the polynomial.

A test program was devised to evaluate the effect of the fraction of penetration depth used when fitting a polynomial by computing the accuracy of the polynomial in predicting the temperature gradient at the l-v interface. The temperature and temperature gradient obtained with the above procedure are compared with the analytical values for a single step change in surface temperature, being the most severe test possible.

Figure 4 gives the relative errors in the surface temperature gradient while Figure 5 gives the relative errors in the surface temperature itself, as a function of the fraction of the penetration depth within which the six equally spaced nodes are located. These computations were also carried out with the first, second, and third order curves of Equation (49). With the nodes contained within a region of 10% of the penetration depth from the surface and using a third order polynomial, the error in the temperature gradient at the interface is less than 0.5%.

3. Combined Liquid-Vapor Region

The basic equation used to solve for the transient states within the tank venting vapor only and containing liquid and vapor initially at a uniform temperature and pressure is given by Equation (28). The states of the vapor within the tank and the liquid arising from condensation from the vapor state are always at a uniform temperature, whereas the temperature distribution within the liquid will vary in accordance with the solution for a semi-infinite solid, as described in the previous section. The system pressure is taken as uniform but time varying.

Solving Equation (28) for the time step dt, and substituting for $\dot{m}_e$ from Equation (20):

$$dt = \frac{m_\sigma}{(h_{g\sigma}-u_\sigma)} \frac{du_\sigma}{\left[\dot{m}_i - K_1 \frac{P_v}{T_v^{1/2}}\right]} \tag{53}$$

$\dot{m}_i$ is determined from Equations (31) and (48), expressions involving u_σ and $h_{g\sigma}$ are given by Equations (11) and (12), m_σ is given by Equations (24) and (25), and P_v can be expressed in terms of the T_v with the Clausius-Clapyron equation or the vapor pressure curve. Temperature of the vapor (and hence the liquid-vapor interface) is used as the computational variable on the right hand side of Equation (53), with time being the dependant variable to be integrated. The quality X, resulting from condensation in the vapor space during the expansion process, must be solved at each computational step by trial-and-error such that Equation (9) is satisfied at each state along the path. It is this element of the solution process that constitutes a major portion of the computational time.

III. RESULTS

The flow sheet is given in Appendix A, while the symbol and program listings are given in Appendices B and C, respectively.

For purposes of comparisons of the computational results using different temperature steps in the expansion process, it is necessary to use specific input parameters at this stage. The experimental parameters used in [9] with R-11 will be used here, and permit comparisons between the measurements of system pres-

sure at the end of the three second vent period and that predicted by the analysis developed here.

Table 2 lists the experimental parameters from [9], along with the final pressure measured after venting for three seconds. The acrylic plastic cylindrical container was 6 cm inside diameter by 10 cm inside length, and had a zero contact angle with R-11. Under the microgravity conditions during free fall sufficient time was allowed for the interface to achieve its equilibrium hemispherical shape before venting was initiated. This serves to define the surface area from which evaporation can take place. Also listed in Table 2 are the final pressures computed by the analysis in [9] and by the analysis presented here. These differ in how the condensation from the vapor space is treated, and in how the mass transfer at the liquid-vapor interface is computed.

It is noted in Table 2 that although minor variations exist in the degree of initial filling and in the initial states, the major differences between the test runs is that the venting orifice diameter increases progressively, which corresponds to an increase in the venting rate expressed in the fourth column as computed initial ullage volumes per second. The tabulated measured and analytic relative pressure drops are the pressure decreases taking place in three seconds divided by the initial system pressure.

The parameters of system pressure, the corresponding saturation temperature, vapor space quality, and mass rates being vented and evaporated at the liquid-vapor interface are plotted in Figures 6-10, corresponding to test numbers 1-5 in Table 2, as

a function of time up to a three second maximum period, using constant step changes in vapor state temperature of $0.5^{o}F$ for the integration of Equation (53).

Results obtained with different degrees and sequences of step changes in temperature during the expansion process are presented in Tables 3-7, corresponding to test numbers 1-5 in Table 2. All computational results presented here were performed with the Harris-800 computer, which has 6 megabytes of virtual address space, handles 10^{6} instructions/second with 24 bits/word and a floating point processor. The objective of varying the computational step changes of temperature was to examine its influence on the results. The smallest constant step used, Computer Runs B with $0.05^{o}F$, give the largest final pressure for all cases. This is not necessarily the most accurate result, because of the accumulation of errors associated with the long computational period required for this case. The largest computational step used, computer Runs A with $0.5^{o}F$, appear to give satisfactory results and were those used to make the plots of Figures 6-10.

IV. DISCUSSION

It is noted in Figures 6-10 that as the initial venting rate increases, as a result of the larger orifice sizes, that the pressure decreases more rapidly, that the evaporation rate increases correspondingly because of the associated decrease in the liquid-vapor interface temperature, and that the evaporation and venting rates approach each other. In Run Number 5 (Figure 10)

the evaporation rate reaches a maximum and then begins to decrease, as a result of the lower rate of pressure decrease, which in turn affects the temperature gradient in the liquid at the liquid-vapor interface.

From Table 2 it is noted that the final pressure computed with the procedure developed here gives somewhat higher pressures than in the analytic results of [9]. This is believed to represent a more accurate result, because of the more accurate computation of the transient temperature gradient at the liquid-vapor interface. Both computed final pressures are significantly lower than the experimental measured ones. This is attributed to neglecting, in the analysis, the evaporation taking place at the meniscus shown in Figure 2, which can be considerable. Additional evaporation would tend to reduce the pressure decrease rate.

V. FUTURE WORK

1. The results presented here should be placed in a generalized form so as to be more generally useful.
2. The analysis should be extended to include evaporation taking place at the solid-vapor-liquid contact line.
3. Investigations should be initiated on the parameters which govern the limits on the pressure decrease rate so as to prevent nucleation. For example, it is noted in Figure 10 that the saturation temperature changes by about $73^{\circ}F$ in three seconds. This means that if the container were sufficiently large and contained a significant amount of liquid,

the liquid would become superheated by this 73°F, and most certainly would nucleate, with local boiling taking place most likely on the walls.

4. Experiments should be conducted with large size containers, to study effects of wall heat capacities, interface areas, and to corroborate the influence of meniscus evaporation.

VI. NOMENCLATURE

a	Thermal Diffusivity
A	Area
C_D	Flow Coefficient
C_v^o	Ideal Gas (low pressure) Specific Heat at Constant Volume
d	Differential
h	Enthalpy
h_{fg}	Latent Heat of Vaporization
k	Thermal Conductivity
K	Constant Defined Locally
K_D	see Equation (22)
m	Mass
P	Pressure
q	Heat Transfer Rate
R	Gas Constant
s	Time as Integration Variable - Equation (38)
S	Entropy
t	Time
T	Temperature

u	Specific Internal Energy
v	Specific Volume
x	Coordinate
X	Quality
γ	Ratio of Specific Heats
δ	Boundary Layer Thickness, Differential
θ	Relative Temperature
ϕ	Dimensionless Temperature
ψ	Dimensionless Temperature Solution for Unit Temperature Disturbance

Subscripts:

e	Exiting Control Volume
f	Liquid
g	Vapor
i	Entering Control Volume
v	Vapor
σ	Control Volume
sat	Saturated Conditions

VII. FIGURES

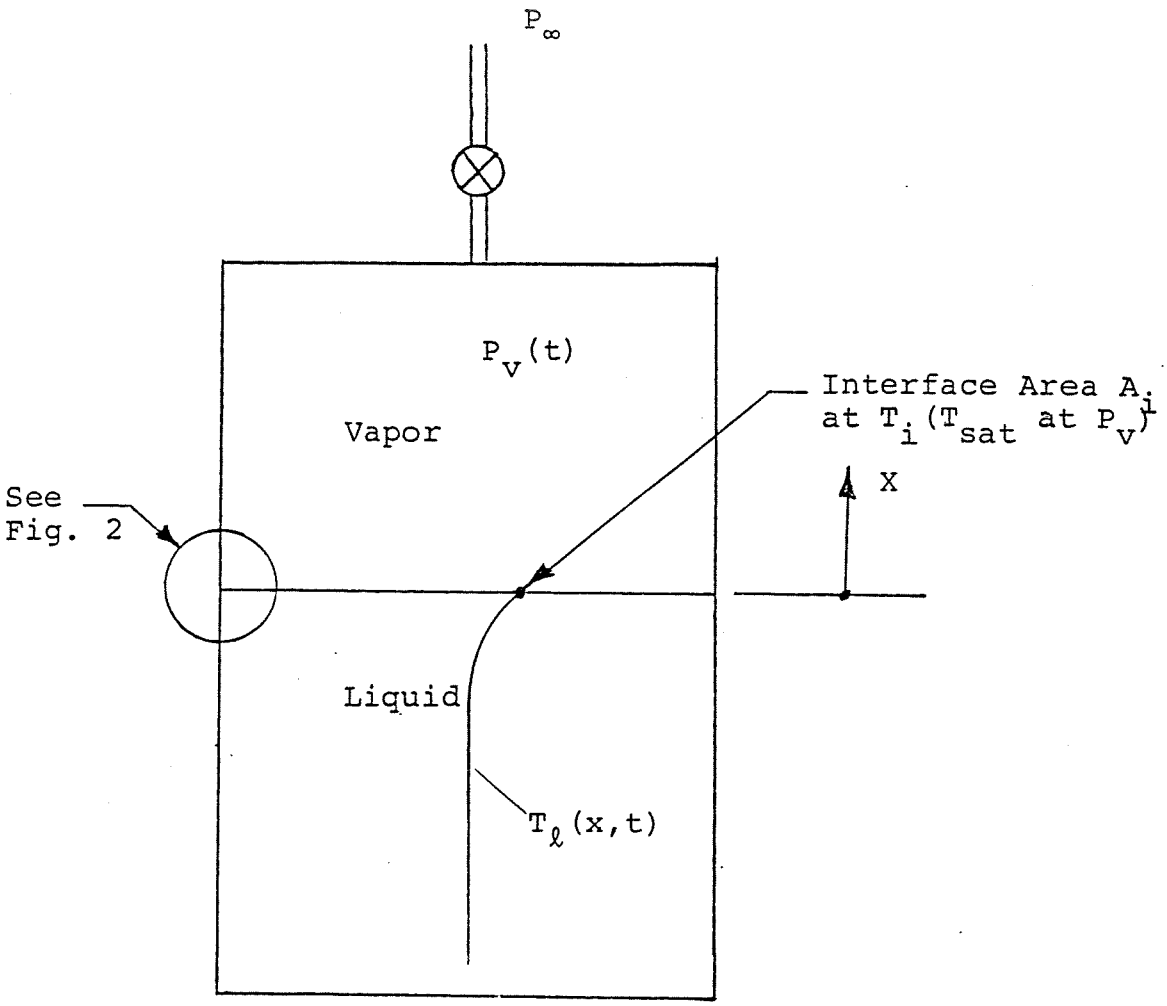

Fig. 1. Schematic of venting system.

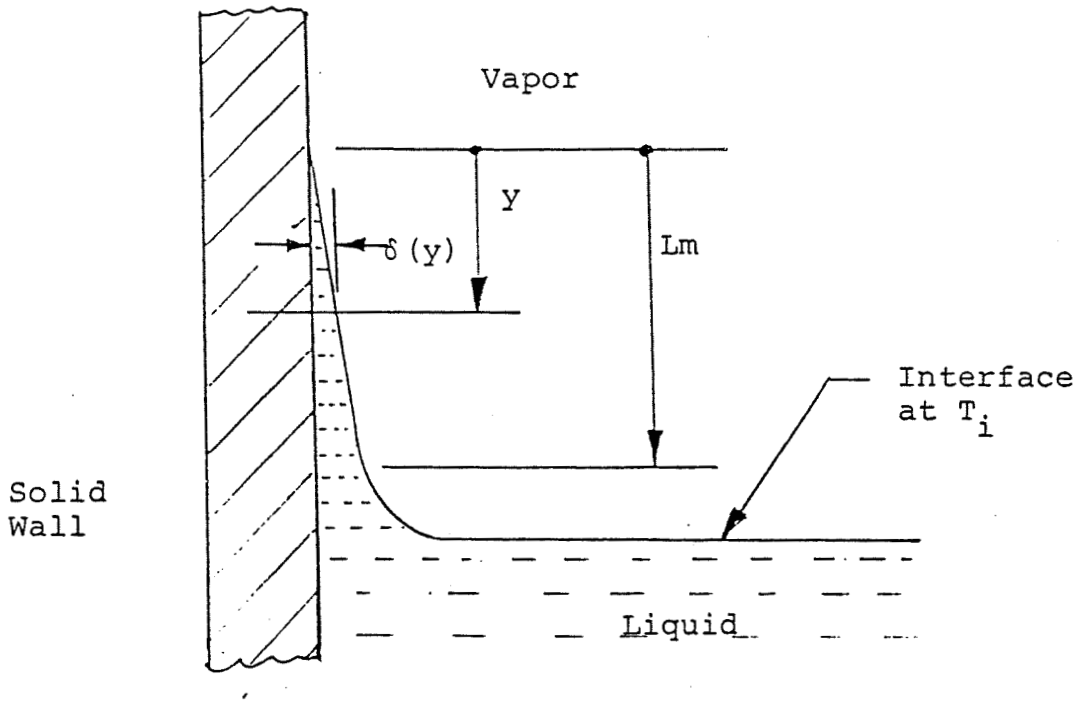

Fig. 2. Detail of Meniscus

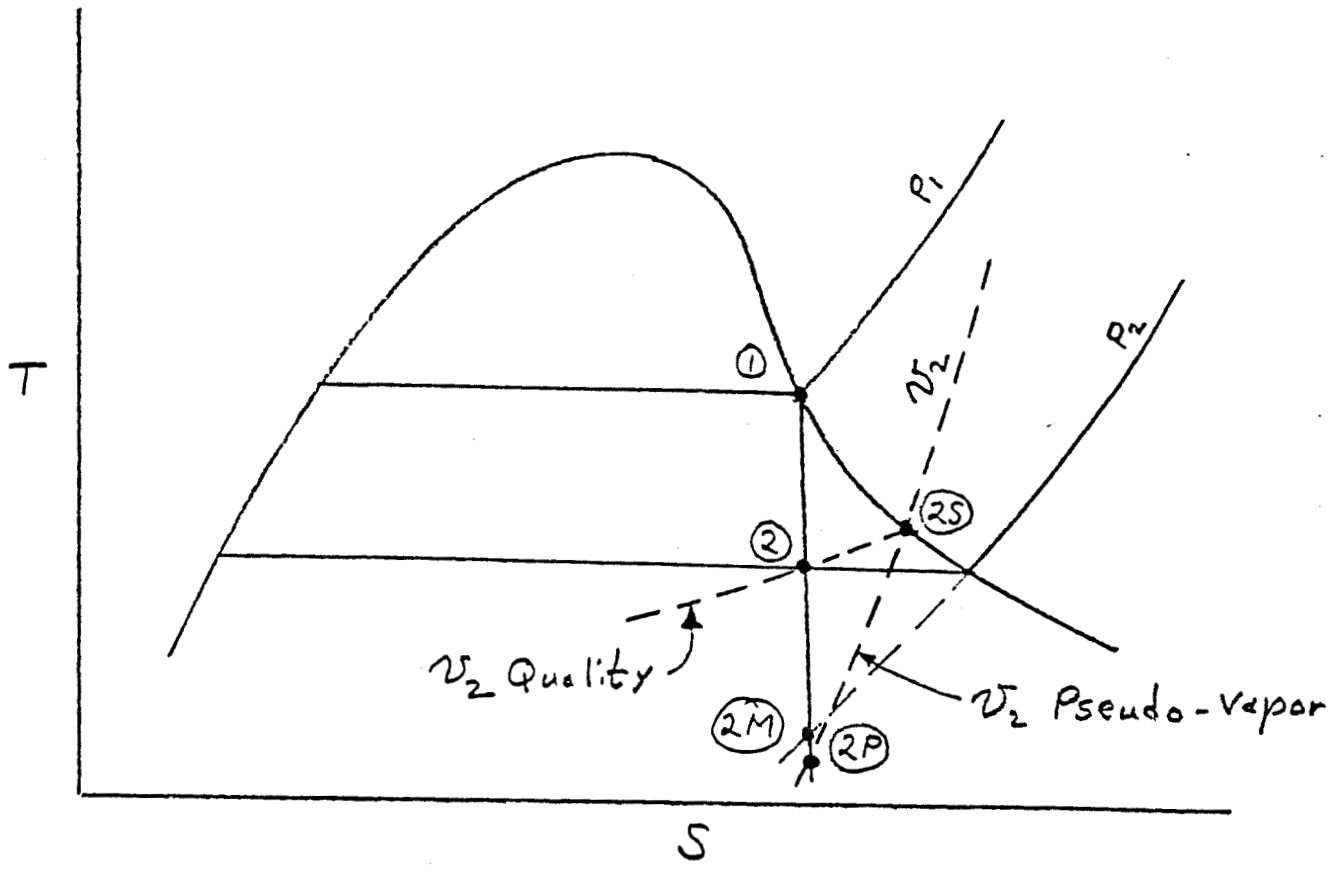

Fig. 3. Isentropic Expansion of Initially Saturated Vapor with Equilibrium Quality and as Pseudo-Vapor.

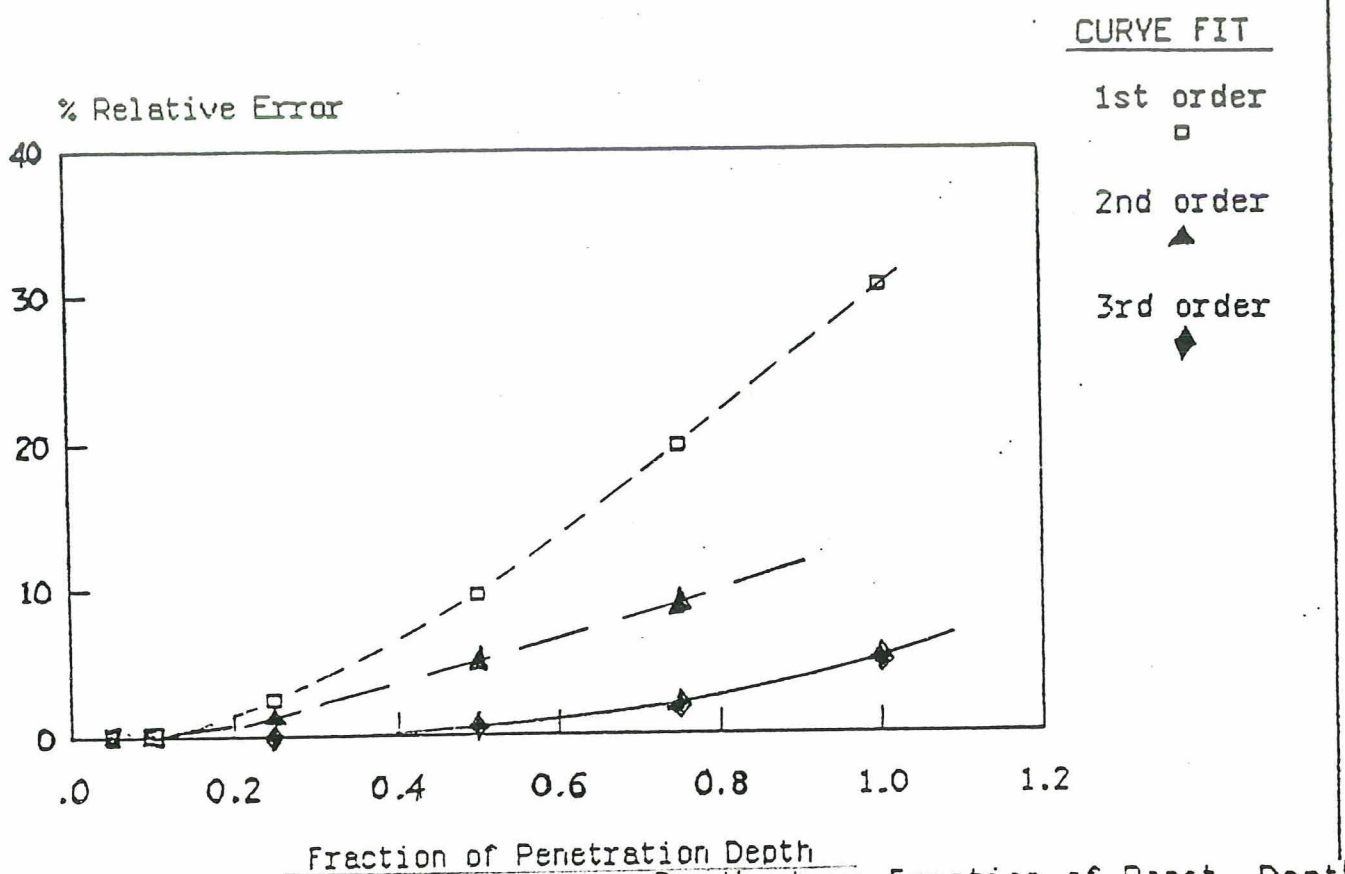

Fig. 4. Error in Surface Temperature Gradient vs Fraction of Penet.. Depth

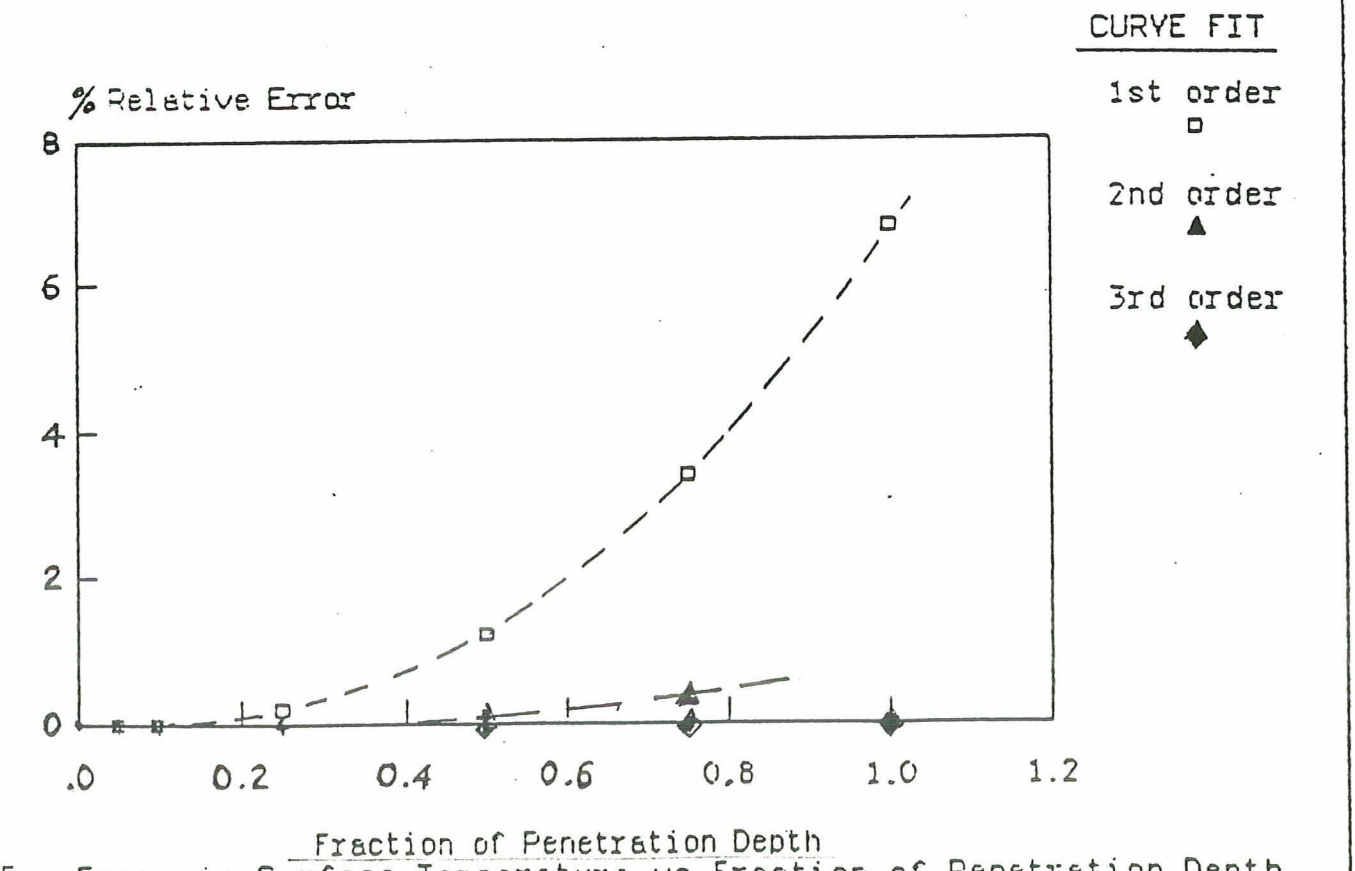

Fig. 5. Error in Surface Temperature vs Fraction of Penetration Depth

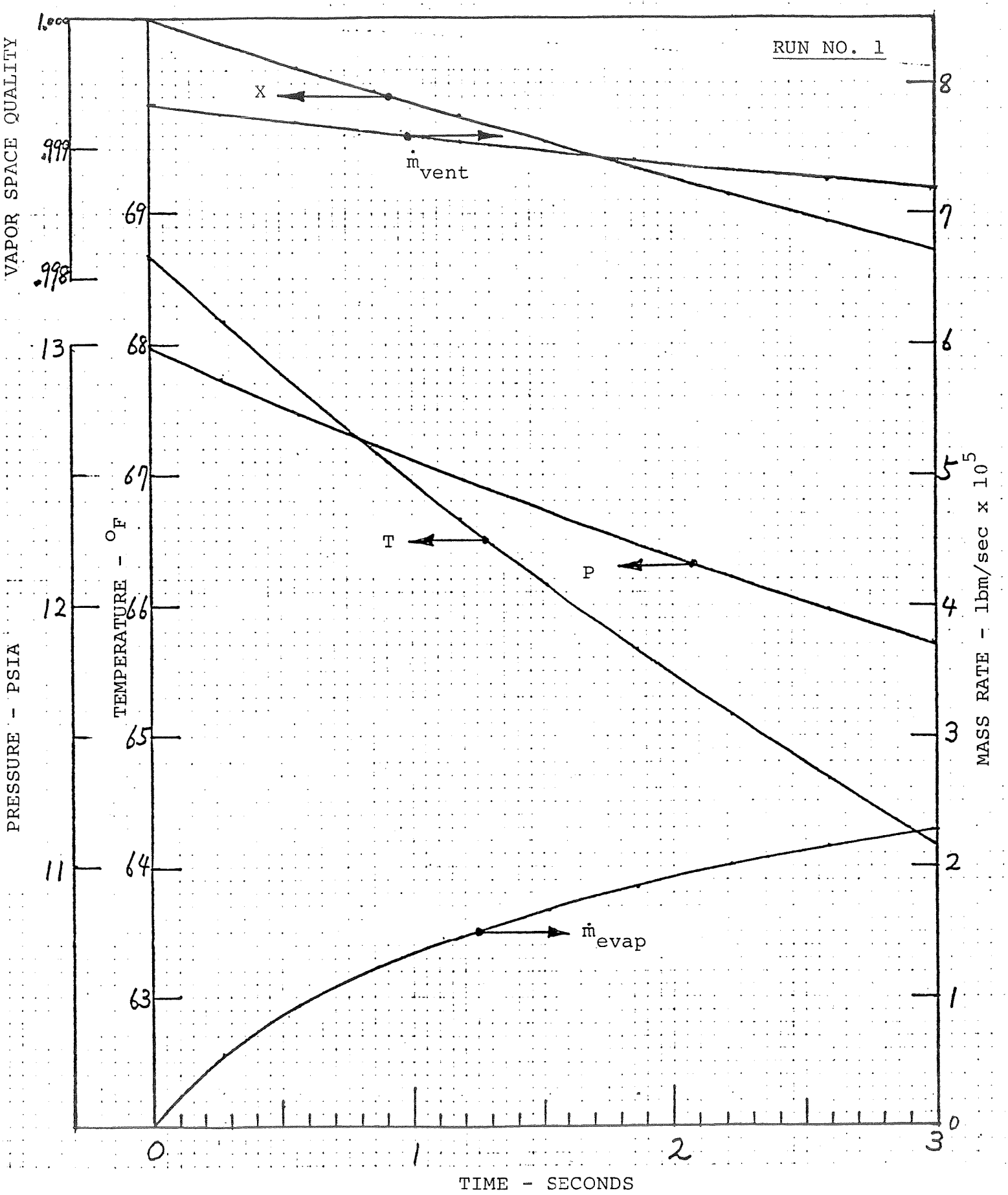

Fig. 6. Computed results for Run No. 1 in Table 2.

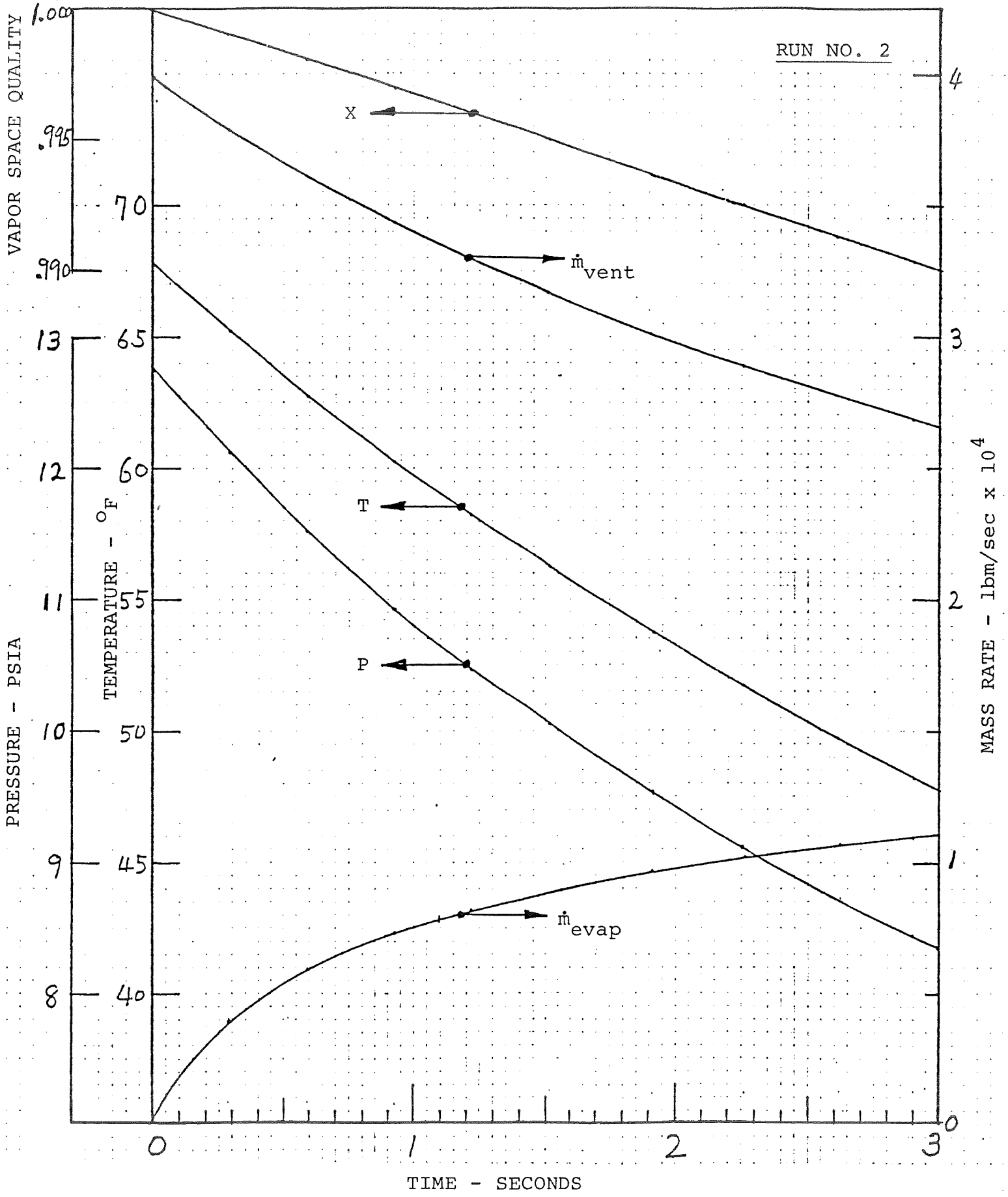

Fig. 7. Computed results for Run No. 2 in Table 2.

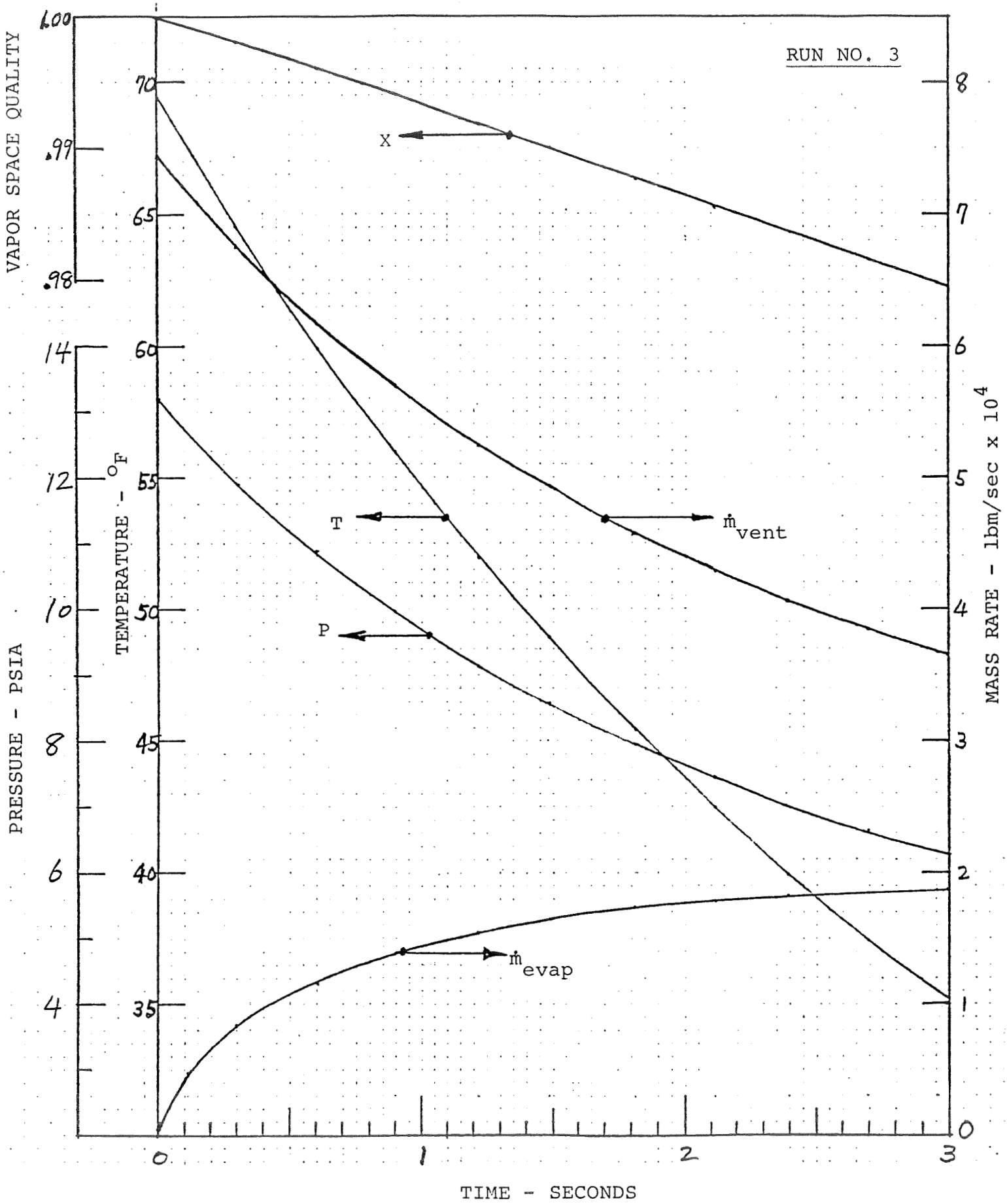

Fig. 8. Computed results for Run No. 3 in Table 2.

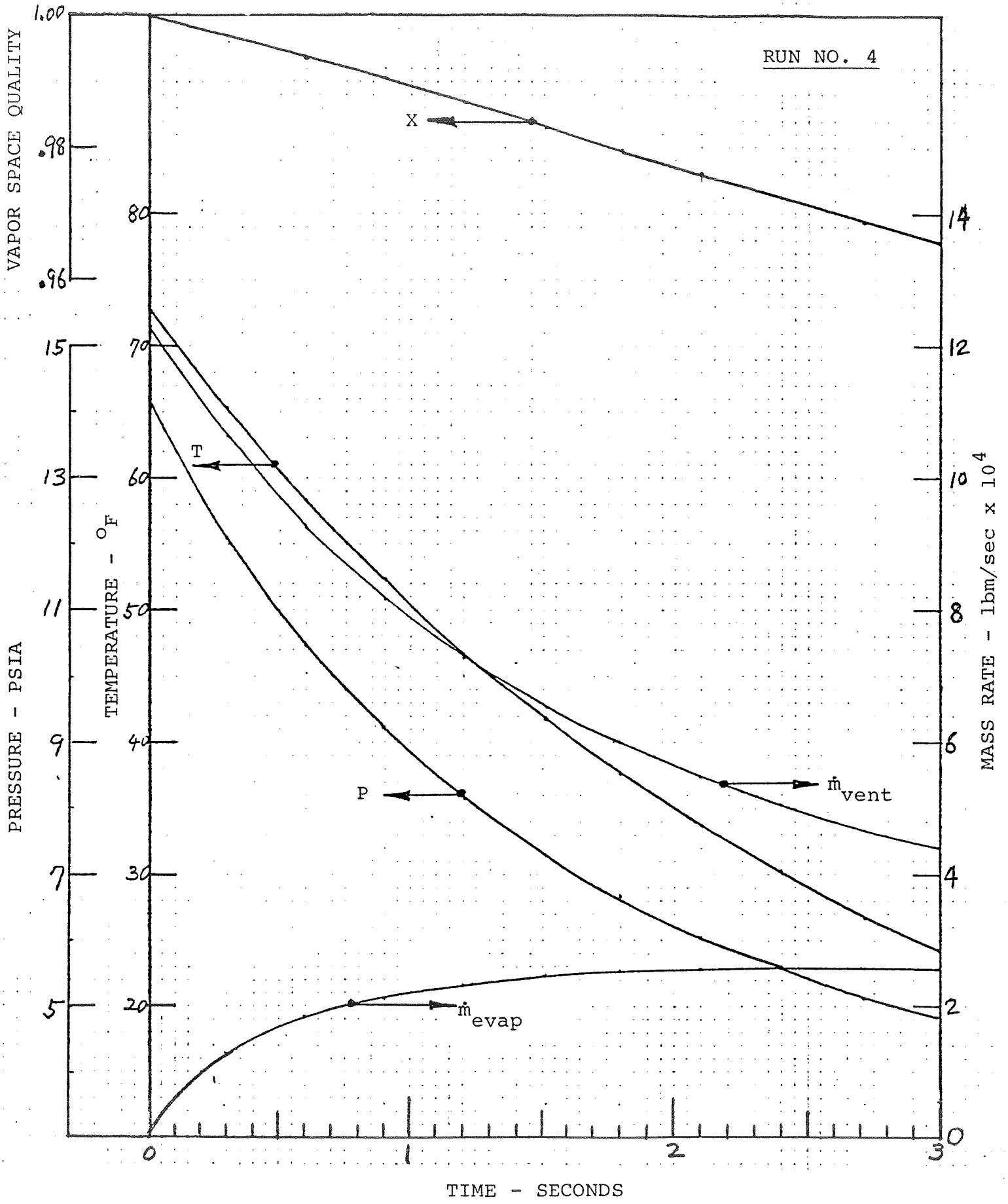

Fig. 9. Computed results for Run No. 4 in Table 2.

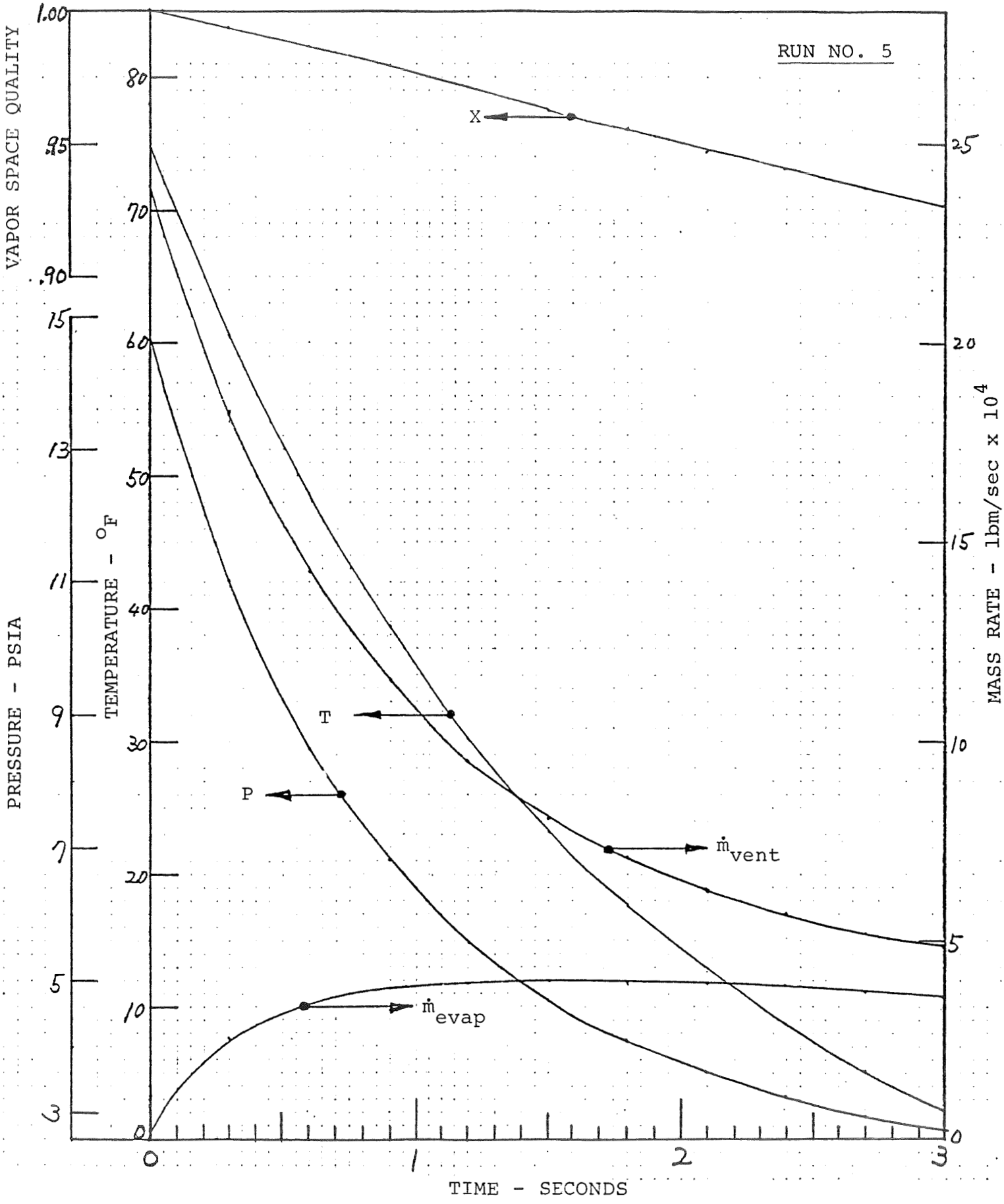

Fig. 10. Computed results for Run No. 5 in Table 2.

VIII. TABLES

Table 1. Computation of final state for venting Freon-11 to one-half the initial mass.

Initial State	Case	Final State		
		T(^{o}F)	P(psia)	X
T = 74.000^{o}F	A	38.300	6.754	.9854
P = 14.447 psia	B	29.138	6.715	-----
X = 1.0000	C-2	37.989	6.705	.9792
T = 160.000^{o}F	A	112.208	28.938	.9943
P = 60.451 psia	B	109.202	28.913	-----
X = 1.0000	C-1	112.028	28.864	.9920
	C-2	112.085	28.892	.9928

Table 2. Experimental Parameters from Reference 9.

Vessel: Acrylic Plastic - 2.36 in (6 cm) I.D. x 3.94 in (10 cm) long

Fluid: R-11 ($CC\ell_3F$)

Inside Volume: 17.33 in^3 (2.84×10^{-4} m^3)

Venting Time: 3 seconds

Test No.	% Initial Vapor Volume	Nozzle Dia. In.	Discharge Coeff. C_D	Reduced Flow Rate Ullage/Sec	Initial Pressure psia	Initial Temp. °F	Final Measured Pressure Drop	Relative Measured Pressure Drop	Final Analytic Pressure (Ref. 9) psia	Relative Analytic Pressure Drop	Final Pressure Computed Here Figs. 6-10 psia
1	68	0.016	0.64	0.035	13.00	70.07	12.50	0.04	11.83	0.09	11.85
2	71	0.035	0.69	0.17	12.75	70.79	10.20	0.20	8.17	0.36	8.36
3	67	0.042	0.86	0.33	13.20	68.99	8.80	0.33	5.90	0.55	6.27
4	68	0.052	0.875	0.51	14.10	74.03	7.80	0.45	4.26	0.70	4.82
5	68	0.076	0.77	1.12	14.65	72.05	6.00	0.59	1.90	0.87	2.71

Table 3. Computer Runs for Test Number 1 in Reference 9.

Computer Run No.	Temperature Steps	Final Values at 3 Sec.			
		P	X	$\dot{m}_{vent}$	$\dot{m}_{evap}$
1A	Constant DT = 0.5 F See Figure 6	11.853	.998	$.719E^{-4}$	$.230E^{-4}$
1B	Constant DT = 0.05 F	11.905	.998	$.722E^{-4}$	$.256E^{-4}$
1C	9 Steps DT = 0.05 F then remaining DT = 1 F	11.838	.998	$.718E^{-4}$	$.214E^{-4}$
1D	Geometric Series Init. DT = .025F Ratio = 1.05	11.890	.998	$.721E^{-4}$	$.241E^{-4}$
1E	Same as D, but DT_{max} = 1.0 F	11.890	.998	$.721E^{-4}$	$.241E^{-4}$
1F	Geometric Series Init. DT = .05 F Ratio = 1.05	11.886	.998	$.721E^{-4}$	$.240E^{-4}$
1G	Same as F, but DT_{max} = 1.0 F	11.886	.998	$.721E^{-4}$	$.240E^{-4}$

Table 4. Computer Runs for Test Number 2 in Reference 9.

Computer Run No.	Temperature Steps	Final Values at 3 Sec.			
		P	X	$\dot{m}_{vent}$	$\dot{m}_{evap}$
2A	Constant DT = 0.5 F See Figure 7	8.361	.990	$.266E^{-3}$	$.111E^{-3}$
2B	Constant DT = 0.05 F	8.454	.990	$.269E^{-3}$	$.116E^{-3}$
2C	9 Steps DT = 0.05 F then remaining DT = 1 F	8.312	.990	$.265E^{-3}$	$.107E^{-3}$
2D	Geometric Series Init. DT = .025F Ratio = 1.07	8.340	.990	$.266E^{-3}$	$.106E^{-3}$
2E	Same as D, but DT_{max} = 1.0 F	8.345	.990	$.266E^{-3}$	$.107E^{-3}$
2F	Geometric Series Init. DT = .05 F Ratio = 1.07	8.337	.990	$.265E^{-3}$	$.106E^{-3}$
2G	Same as F, but DT_{max} = 1.0 F	8.342	.990	$.266E^{-3}$	$.107E^{-3}$

Table 5. Computer Runs for Test Number 3 in Reference 9.

Computer Run No.	Temperature Steps	Final Values at 3 Sec.			
		P	X	$\dot{m}_{vent}$	$\dot{m}_{evap}$
3A	Constant DT = 0.5 F See Figure 8	6.269	.979	$.365E^{-3}$	$.187E^{-3}$
3B	Constant DT = 0.06 F	6.364	.980	$.370E^{-3}$	$.194E^{-3}$
3C	9 Steps DT = 0.06 F then remaining DT = 1 F	6.213	.979	$.362E^{-3}$	$.184E^{-3}$
3D	Geometric Series Init. DT = .03 F Ratio = 1.06	6.203	.979	$.361E^{-3}$	$.178E^{-3}$
3E	Same as D, but DT_{max} = 1.0 F	6.232	.979	$.363E^{-3}$	$.183E^{-3}$
3F	Geometric Series Init. DT = .06 F Ratio = 1.06	6.203	.979	$.361E^{-3}$	$.178E^{-3}$
3G	Same as F, but DT_{max} = 1.0 F	6.230	.979	$.363E^{-3}$	$.183E^{-3}$

Table 6. Computer Runs for Test Number 4 in Reference 9.

Computer Run No.	Temperature Steps	Final Values at 3 Sec.			
		P	X	$\dot{m}_{vent}$	$\dot{m}_{evap}$
4A	Constant DT = 0.5 F See Figure 9	4.822	.966	$.439E^{-3}$	$.258E^{-3}$
4B	Constant DT = 0.06 F	4.909	.966	$.447E^{-3}$	$.266E^{-3}$
4C	9 Steps DT = 0.06 F then remaining DT = 1 F	4.771	.965	$.435E^{-3}$	$.254E^{-3}$
4D	Geometric Series Init. DT = .03 F Ratio = 1.04	4.757	.965	$.434E^{-3}$	$.249E^{-3}$
4E	Same as D, but DT_{max} = 1.0 F	4.784	.965	$.436E^{-3}$	$.254E^{-3}$
4F	Geometric Series Init. DT = .06 F Ratio = 1.04	4.757	.965	$.434E^{-3}$	$.248E^{-3}$
4G	Same as F, but DT_{max} = 1.0 F	4.783	.965	$.436E^{-3}$	$.254E^{-3}$

Table 7. Computer Runs for Test Number 5 in Reference 9.

Computer Run No.	Temperature Steps	Final Values at 3 Sec.			
		P	X	$\dot{m}_{vent}$	$\dot{m}_{evap}$
5A	Constant DT = 0.5 F See Figure 10	2.711	.927	$.476E^{-3}$	$.356E^{-3}$
5B	Constant DT = 0.05 F	2.771	.928	$.486E^{-3}$	$.364E^{-3}$
5C	9 Steps DT = 0.05 F then remaining DT = 1 F	2.677	.926	$.470E^{-3}$	$.351E^{-3}$
5D	Geometric Series Init. DT = .025F Ratio = 1.028	2.656	.925	$.467E^{-3}$	$.346E^{-3}$
5E	Same as D, but DT_{max} = 1.0 F	2.682	.926	$.471E^{-3}$	$.352E^{-3}$
5F	Geometric Series Init. DT = .05 F Ratio = 1.028	2.657	.925	$.467E^{-3}$	$.346E^{-3}$
5G	Same as F, but DT_{max} = 1.0 F	2.682	.926	$.471E^{-3}$	$.352E^{-3}$

IX. REFERENCES

1. Collins, R. L., "Choked Expansion of Subcooled Water and I.H.E. Flow Model," J. Heat Transfer, Trans. ASME, 100, #2, May 1978, pp. 275-280.

2. Levy, S. and Abdollahian, D., "Homogeneous Non-Equilibrium Critical Flow Model," Int., J. of Heat and Mass Transfer, Vol. 25, No. 6, June 1982, pp. 759-770.

3. Winters, W. S. and Merte, H., "Experiments and Nonequilibrium Analysis of Pipe Blowdown," Nuclear Science and Engineering, 69, 1979, pp. 411-429.

4. Moody, F. J., "Maximum Two-Phase Vessel Blowdown from Pipes," J. of Heat Transfer, Vol. 88, No. 3, August 1966, pp. 285-295.

5. Moody, F. J., "Liquid/Vapor Action in a Vessel During Blowdown," J. Engineering for Power, Trans. ASME, Vol. 91, No. 1, Ser. A, January 1969, pp. 53-61.

6. Eberhart, J. G., "The Thermodynamic and the Kinetic Limits of Superheat of a Liquid," J. Colloid and Interface Science 56, 2, August 1976, pp. 262-269.

7. Semenova, N. M. and Yermakov, G. V., "The Limit of Thermodynamic Stability of Single-Phase Liquids," Heat Trans. Soviet Res. 11, 6, November/December 1979, pp. 75-78.

8. Miyatake, O., et al, "Flash Evaporation Phenomena of Pool Water," Heat Transfer-Japanese Research 6, 2, April/June 1977, pp. 13-24.

9. Labus, T. L.; Aydelott, J. C.; Amling, G. E.; "Zero Gravity Venting of Three Refrigerants," NASA TN D-7480, 1974.

10. Wayner, P. C., Jr., Kao, Y. K., and LaCroix, L. V., "The Interline Heat-Transfer Coefficient of an Evaporating Wetting Film," Int. J. Heat Mass Transfer, 19 #5, May 1976, pp. 487-492.

11. Merte, H., Jr., "Condensation Heat Transfer," Chapter in Vol. 9, Advances in Heat Transfer, ed. by T. Irvine, Jr. and J. P. Hartnett, Academic Press, 1973, pp. 181-222.

12. "Thermodynamic Properties of Freon-11 Refrigerant (Trichlorofluoromethane)," Publication T-11, E. I. DuPont de Nemours and Co. (Inc.), Wilmington, Del., 1965.

13. White, Frank M., Fluid Mechanics, 1979, McGraw-Hill, Inc. New York, pp. 530-531.

14. Arpaci, Vedat S., Conduction Heat Transfer, Addison Wesley Publishing Company, 1966.

15. Burden, Richard L., Faires, Douglas J., and Reynolds, Albert C., Numerical Analysis, Pridle, Weber, & Schmidt, 1981, pp. 250-258, 319-326.

Appendix A. Algorithm Flow Chart

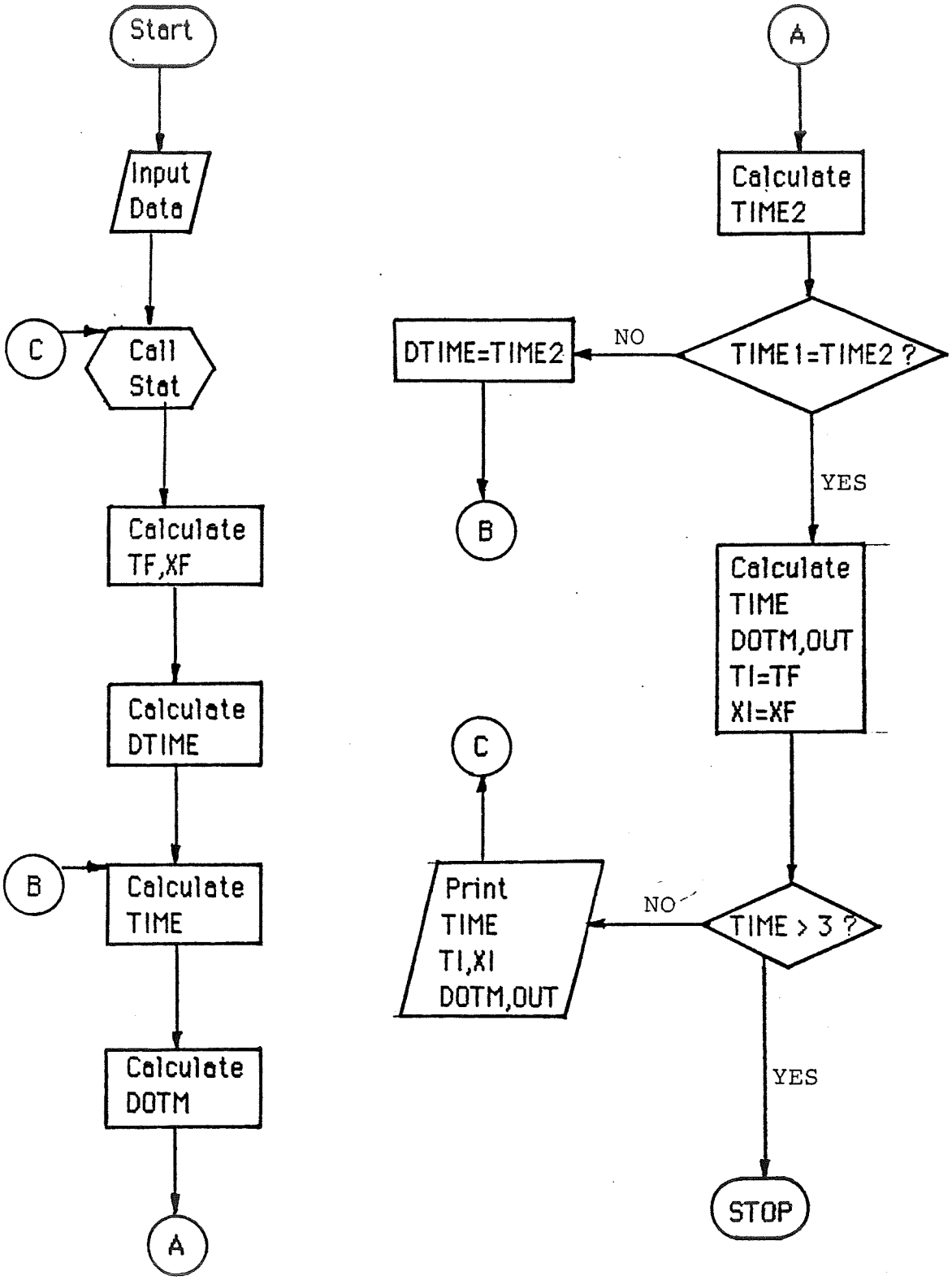

Appendix B. Symbol Listing

FORTRAN Symbol	Description	Units
AIN	Total mass of evaporated vapor	Lbm
AOUT	Total mass of vented vapor	Lbm
AMASS	Initial mass of vapor domain	Lbm
AS	Interface surface area	in^2
AT	Nozzle corss sectional area	in^2
CD	Discharge coefficient	-
COND	Thermal conductivity of liquid @T	$Btu/hr\text{-}ft\text{-}^oF$
CV	Constant volume spcecific heat of vapor @T	$Btu/Lbm\ ^oF$
CP	Constant pressure specific heat of vapor @T	$Btu/Lbm\ ^oF$
DOTM	Mass flow rate across interface	Lbm/Sec
DT,DTEMP	Temperature step	^oF
DTIME	Time step	Seconds
DTR	Temperature ratio	-
HF	Enthalpy of saturated liquid @T	Btu/Lbm
HG	Enthalpy of saturated vapor @T	Btu/Lbm
OUT	Mass flow rate of vented vapor	Lbm/Sec
PSAT	Saturation pressure @T	Psia
SF	Entropy of saturated liquid @T	$Btu/Lbm\ ^oF$
SG	Entropy of saturated vapor @T	$Btu/Lbm\ ^oF$
T	Temperature	^oR
TF	Final ullage temperature at next step	^oR
TI	Initial ullage temperature	^oR
TIME	Total elapsed time	Seconds
TIME2	Elapsed time for each step	Seconds
TO	Initial ullage temperature	^oF
UF	Internal energy of saturated liquid @T	Btu/Lbm
UG	Internal energy of saturated vapor @T	Btu/Lbm
VF	Specific volume of saturated liquid @T	Ft^3/Lbm
VG	Specific volume of saturated vapor @T	Ft^3/Lbm
XF	Final quality of vapor at next step	-
XI	Initial quality of vapor	-

Appendix C. Program Listing

```
      DIMENSION DTIME(1000),DTEMP(1000),CDD(5),ATT(5),AMASSS(5),
     *TOO(5),DTT(5),DTRR(5)
C  DISCHARGE COEFFICIENT
      DATA CDD/.64,.69,.86,.875,.77/
C  AREA OF VENT NOZZLE AT THROAT IN SQUARE IN
      DATA ATT/2.00866E-4,9.6211E-4,1.39376E-3,2.121141E-3,
     *4.534571E-3/
C  INITIAL VAPOR MASS IN LBM
      DATA AMASSS/2.2252411E-3,2.2765134E-3,2.2225181E-3,
     *2.4005919E-3,2.4879826E-3/
C  INITIAL ULLAGE TEMPERATURE IN DEG F
      DATA TOO/68.6795,67.730,69.451,72.780,74.707/
C  INITIAL TEMPERATURE STEP IN DEG F
      DATA DTT/.05,.05,.06,.06,.05/
C  TEMPERATURE RATIO
      DATA DTRR/1.05,1.07,1.06,1.04,1.028/
C  LIQUID-VAPOR INTERFACE AREA IN SQUARE IN
      AS=8.6303608
C  RUN 5 TIMES BASED ON 5 EXPERIMENTAL DATA(INPUT)
      DO 1 L=1,5
C  PRINT RUN NUMBER, INITIAL TEMP, TEMP RATIO
      WRITE(20,500)
      WRITE(20,600)L,DTT(L),DTRR(L)
C  SET INITIAL QUALITY OF VAPOR DOMAIN
      XI=1.
C  SET DISCHARGE COEFFICIENT
      CD=CDD(L)
C  SET AREA OF VENT NOZZLE AT THROAT
      AT=ATT(L)
C  SET INITIAL VAPOR MASS
      AMASS=AMASSS(L)
C  SET INITIAL ULLAGE TEMPERATURE
      TO=TOO(L)
C  SET INITIAL TEMPERATURE STEP
      DT=DTT(L)
C  SET TEMPERATURE RATIO
      DTR=DTRR(L)
C  PRINT HEADING
      WRITE(20,100)
C  PRINT UNITS OF INPUT AND OUTPUT
      WRITE(20,300)
C  INITIAL TEMP FROM FAHRENHEIT TO RANKINE
      TI=TO+459.67
C  TOTAL ELAPSED TIME
      TIME=0.
C  INITIAL MASS FLOW RATE ACROSS LIQUID-VAPOR INTERFACE
      DOTM1=0.
C  TOTAL MASS OF VAPOR ACROSS LIQUID-VAPOR INTERFACE
      AIN=0.
C  TOTAL MASS OF VENTED VAPOR
      AOUT=0.
C
```

```
C  PRINT INITIAL INPUT
C
C  TIME=TOTAL ELAPSED TIME IN SECOND
C  TO=TEMPERATURE IN FAHRENHEIT
C  PSAT=CORRESPONDING SATURATED PRESSURE IN PSIA
C  XI=QUALITY OF VAPOR DOMAIN
C  AMASS=MASS OF VAPOR DOMAIN IN LBM
C  DOTM1=MASS FLOW RATE ACROSS LIQUID-VAPOR INTERFACE IN LBM/SEC
C  OUT=MASS FLOW RATE OF VENTED VAPOR IN LBM/SEC
C  AIN=TOTAL MASS OF VENTED VAPOR IN LBM
C  AOUT=TOTAL MASS OF VAPOR ACROSS LIQUID-VAPOR INTERFACE IN LBM
C
      WRITE(20,200)TIME,TO,PSAT(TI),XI,AMASS,DOTM1,OUT(TI,CD,AT)
     *,AIN,AOUT
C
C  SET ALL TIME STEPS AND TEMPERATURE STEPS ZERO
      DO 6 J=1,1000
      DTIME(J)=0.
      DTEMP(J)=0.
    6 CONTINUE
C
      K=2
    2 CALL STAT(TI,XI,DT,TF,XF,A)
      DOTM2=0.
      DTIME(K)=VENT(TI,XI,TF,XF,CD,AT,AMASS,A*AMASS)
      TIME1=TIME+DTIME(K)
      DTEMP(K)=DT
    4 DO 5 I=2,K
      TIME1=TIME1-DTIME(I-1)
      DOTM2=DOTM2+EVAP(TF,DTEMP(I),AS,TIME1)
    5 CONTINUE
      TIME2=AVENT(TI,XI,TF,XF,CD,AT,AMASS,A*AMASS,DOTM1,DOTM2)
      TOL=TIME2*.00001
      IF(ABS(TIME1-TIME2).LT.TOL)THEN
      GO TO 3
      ELSE
      DOTM2=0.
      TIME1=TIME+TIME2
      GO TO 4
      ENDIF
    3 DTIME(K)=TIME2
      AIN=AIN+(DOTM1+DOTM2)*.5*DTIME(K)
      AOUT=AOUT+(OUT(TI,CD,AT)+OUT(TF,CD,AT))*.5*DTIME(K)
      TIME=TIME+DTIME(K)
      TI=TF
      XI=XF
      DOTM1=DOTM2
      K=K+1
      AMASS=A*AMASS
      DT=DT*DTR
      IF(DT.GT.1.)THEN
```

```
      DT=1.
      GO TO 3
    2 DT=DT
      ENDIF
      WRITE(20,200)TIME,TF-459.67,PSAT(TF),XF,AMASS,DOTM1,
     *COUT(TF,CD,AT),AIN,AOUT
      IF(TIME.GT.3.0)GO TO 1
      GO TO 2
    1 CONTINUE
  100 FORMAT(//,4X,'TIME',4X,'TSAT',5X,'PSAT',5X,'QTY',6X,'VAP MASS',
     *6X,'EVAP RATE',5X,'VENT RATE',5X,'MASS EVAP',5X,'MASS VENT',/)
  200 FORMAT(2X,F8.5,1X,F8.4,1X,F9.5,1X,F7.5,5(2X,E12.6))
  300 FORMAT(4X,'(SEC)',3X,'(DEG F)',2X,'(PSIA)',12X,'(LBM)',9X,
     *'(LBM/SEC)',5X,'(LBM/SEC)',/)
  500 FORMAT(////,4X,'RUN #',7X,'INIT TSTEP',6X,'TRATIO')
  600 FORMAT(6X,I1,10X,F6.4,10X,F5.3)
      STOP
      END
C
C
C  FUNCTION COND CALCULATES THERMAL CONDUCTIVITY OF LIQUID
C  FREON-11 AS A FUNCTION OF TEMPERATURE
C  CONDUCTIVITY IS IN BTU/(HR)(FT)(DEG F)
C  TEMPERATURE IS IN DEG RANKINE
C
      FUNCTION COND(T)
      IF(T.LT.419.67)THEN
      COND=.0633
      ELSEIF(T.LT.459.67)THEN
      COND=.0633+(.0587-.0633)*(T-419.67)/40.
      ELSEIF(T.LT.479.67)THEN
      COND=.05874(.0540-.0587)*(T-459.67)/40.
      ELSEIF(T.LT.579.67)THEN
      COND=.0540+(.0449-.0540)*(T-479.67)/20.
      ELSE
      COND=.0449
      ENDIF
      RETURN
      END
C
C
C  FUNCTION EVAP CALCULATES MASS FLOW RATE ACROSS LIQUID-VAPOR
C  INTERFACE DETERMINED FROM CONSERVATION OF ENERGY EQUATION
C  APPLIED TO LIQUID-VAPOR INTERFACE
C  EVAP IS IN LBM/SEC
C  T IS TO CALCULATE PROPERTIES IN DEG RANKINE
C  DELT IS TEMPERATURE DROP AT LIQUID-VAPOR INTERFACE
C  AS IS LIQUID-VAPOR INTERFACE AREA IN IN2
C
      FUNCTION EVAP(T,DELT,AS,TIME)
      EVAP=SQRT(COND(T)*CP(T)/(TIME*VF(T)))*AS*DELT
     */(HG(T)-HF(T))/15314.00127
```

```
      RETURN
      END
C
C
C  FUNCTION VENT CALCULATES TIME WITH EVAPORATION TAKEN BETWEEN
C  2 GIVEN CONDITIONS
C
      FUNCTION VENT(T1,X1,T2,X2,CD,AT,AMASS,BMASS)
      VENT=(RATE(T1,X1,CD,AT,AMASS)+RATE(T2,X2,CD,AT,BMASS))*.5*
     *(UG(T2,X2)-UG(T1,X1))
      RETURN
      END
C
C
C  FUNCTION RATE CALCULATES 1/(dU/dt) INSIDE VAPOR DOMAIN WITH
C  EVAPORATION FOR GIVEN CONDITION
C
      FUNCTION RATE(T,X,CD,AT,AMASS)
      R=.0781164927
      RATE=-AMASS*SQRT(T*R)/(CD*AT*AKD(T)*FUN(T,X)*PSAT(T))*2.11557642
      RETURN
      END
C
C
C  FUNCTION OUT CALCULATES MASS FLOW RATE OF VENTED VAPOR
C  OUT IS IN LBM/SEC
C  T IS IN DEG RANKINE
C  CD IS DISCHARGE COEFFICIENT
C  AT IS AREA OF VENT NOZZLE IN SQUARE IN
C
      FUNCTION OUT(T,CD,AT)
      R=.0781164927
      OUT=PSAT(T)*CD*AT*AKD(T)/(SQRT(T*R)*2.115557642)
      RETURN
      END
C
C  FUNCTION AVENT CALCULATES TIME WITHOUT EVAPORATION TAKEN
C  BETWEEN 2 GIVEN CONDITIONS
C
      FUNCTION AVENT(T1,X1,T2,X2,CD,AT,AMASS,BMASS,DOTM1,DOTM2)
      AVENT=(ARATE(T1,X1,CD,AT,AMASS,DOTM1)
     *+ARATE(T2,X2,CD,AT,BMASS,DOTM2))*.5*(UG(T2,X2)-UG(T1,X1))
      RETURN
      END
C
C
C  FUNCTION ARATE CALCULATES 1/(dU/dt) INSIDE VAPOR DOMAIN
C  WITHOUT EVAPORATION FOR GIVEN CONDITION
      FUNCTION ARATE(T,X,CD,AT,AMASS,DOTM)
      R=.0781164927
      ARATE=-AMASS/FUN(T,X)/(CD*AT*AKD(T)*PSAT(T)/(SQRT(T*R)*
     *2.11557642)-DOTM)
```

```
      RETURN
      END
C
C
C  FUNCTION AKD CALCULATES VALUE OF CONSTANT IN CHOKE FLOW EQUATION
C
      FUNCTION AKD(T)
      GAMMA=CP(T)/CV(T)
      AKD=SQRT(GAMMA)*(2./(GAMMA+1.))**((GAMMA+1.)*.5/(GAMMA-1.))
      RETURN
      END
C
C
C  SUBROUTINE STAT CALCULATES QUALITY AND VOLUME CHANGE OF VAPOR
C  DOMAIN GIVEN INITIAL TEMPERATURE, QUALITY, AND TEMPERATURE
C  DROP
C
      SUBROUTINE STAT(T1,X1,DT,T2,X2,A)
      VOL1=VOL(T1,X1)
      T2=T1-DT
      X2=(S(T1,X1)-SF(T2))/(SG(T2)-SF(T2))
      VALUE1=DIF(T1,X1,T2,X2)
      DX=DT*.00001
    1 X2=X2-DX
      VALUE2=DIF(T1,X1,T2,X2)
      IF (ABS(VALUE1).GT.ABS(VALUE2)) THEN
      VALUE1=VALUE2
      GO TO 1
      ELSE
      X2=X2+DX
      ENDIF
      A=VOL1/VOL(T2,X2)
      RETURN
      END
C
C
C  FUNCTION FUN CALCULATES VALUE OF (HG-U) INSIDE VAPOR DOMAIN
C
      FUNCTION FUN(T,X)
      FUN=(HG(T)-HF(T))*(1.-X)+PSAT(T)*VOL(T,X)*.185053
      RETURN
      END
C
C
C  FUNCTION UG CALCULATES INTERNAL ENERGY INSIDE VAPOR DOMAIN
C
      FUNCTION UG(T,X)
      UG=HG(T)-FUN(T,X)
      RETURN
      END
C
C
```

```
C  FUNCTION VOL CALCULATES VOLUME OF VAPOR DOMAIN
C
      FUNCTION VOL(T,X)
      VOL=X*VG(T)+(1.-X)*VF(T)
      RETURN
      END
C
C
C  FUNCTION S CALCULATES ENTROPY OF VAPOR DOMAIN
C
      FUNCTION S(T,X)
      S=X*SG(T)+(1.-X)*SF(T)
      RETURN
      END
C
C
C  FUNCTION DIF IS USED IN SUBROUTINE STAT TO CALCULATE THE
C  DIFFERENCE IN INTEGRATED VALUES OF 2 EQUATIONS
C
      FUNCTION DIF(T1,X1,T2,X2)
      Z1=(UG(T2,X2)-UG(T1,X1))*.5*(1./FUN(T1,X1)+1./FUN(T2,X2))
      Z2=ALOG(VOL(T1,X1))-ALOG(VOL(T2,X2))
      DIF=Z1-Z2
      RETURN
      END
C
C
C  FUNCTION PSAT CALCULATES SATURATED PRESSURE AT CORRESPONDING
C  TEMPERATURE
C  PSAT IS IN PSIA
C  T IS IN DEG RANKINE
C
      FUNCTION PSAT(T)
      A=42.14702865
      B=-4344.343607
      C=-12.84696753
      D=.0040088372507
      E=.03136605356
      F=862.07
      P1=A+B/T+C*ALOG10(T)+D*T+E*(F-T)/T*ALOG10(F-T)
      PSAT=EXP(ALOG(10.)*P1)
      RETURN
      END
C
C
C  FUNCTION VF CALCULATES VOLUME OF SATURATED LIQUID FREON-11
C  VF IS IN CU FT/LBM
C  T IS IN DEG RANKINE
C
      FUNCTION VF(T)
      A=34.57
      B=57.63811
```

```
      C=47.6322
      D=-42.83356
      E=34.70663
      TC=848.07
      F=1.-T/TC
      DEN=A+B*F**(1./3.)+C*F**(2./3.)+D*F-E*F**(4./3.)
      VP=1./DEN
      RETURN
      END
C
C
C  FUNCTION ANEWTON WILL BE USED IN FUNCTION VG TO FIND
C  ROOT OF EQUATION OF STATE BY USING NEWTON'S METHOD
C
      FUNCTION ANEWTON(T,V)
      R=.078117
      B=.0019
      A2=-3.126759
      B2=.001318523
      C2=-35.76999
      A3=-.025341
      B3=4.875121E-5
      C3=1.220367
      A4=.001687277
      B4=-1.805062E-6
      A5=-2.35893E-5
      B5=2.448303E-8
      C5=-1.478379E-4
      A6=1.057504E2
      B6=-9.472103E4
      TC=848.07
      BK=-4.5
      VP=V-B
      H=BK*T/TC
      P=PSAT(T)
      F=-P+R*T/VP+(A2+B2*T+C2*EXP(H))/VB**2.+
     $(A3+B3*T+C3*EXP(H))/VB**3.+(A4+B4*T)/VB**4.+
     $(A5+B5*T+C5*EXP(H))/VB**5.
      DF=-R*T/VB**2.-2.*(A2+B2*T+C2*EXP(H))/VB**3.-
     $3.*(A3+B3*T+C3*EXP(H))/VB**4.-4.*(A4+B4*T)/VB**5.-
     $5.*(A5+B5*T+C5*EXP(H))/VB**6.
      IF (V.GT..1) GO TO 1
      F=F+(A6+B6*T)/EXP(580.*V)
      DF=DF-580.*(A6+B6*T)/EXP(580.*V)
    1 ANEWTON=F/DF
      RETURN
      END
C
C
C  FUNCTION VG CALCULATES VOLUME OF SATURATED VAPOR FREON-11
C  VG IS IN CU FT/LBM
C  T IS IN DEG RANKINE
```

```
C
      FUNCTION VG(T)
      TF=T-459.67
      IF(TF.LT.-38.)THEN
      VO=50.
      ELSEIF(TF.LT.-14.)THEN
      VO=30.
      ELSEIF(TF.LT.13.)THEN
      VO=15.
      ELSEIF(TF.LT.43.)THEN
      VO=7.
      ELSEIF(TF.LT.92.)THEN
      VO=3.
      ELSEIF(TF.LT.136.)THEN
      VO=1.5
      ELSEIF(TF.LT.188.)THEN
      VO=.7
      ELSEIF(TF.LT.266.)THEN
      VO=.3
      ELSEIF(TF.LT.300.)THEN
      VO=.15
      ELSEIF(TF.LT.330.)THEN
      VO=.11
      ELSE
      VO=.06
      ENDIF
      TOL=VO*1E-4
    1 V1=VO-ANEWTON(T,VO)
      IF(ABS(V1-VO).LT.TOL) GO TO 2
      VO=V1
      GO TO 1
    2 VG=V1
      RETURN
      END
C
C
C  FUNCTION HG CALCULATES ENTHALPY OF SATURATED VAPOR FREON-11
C  HG IS IN BTU/LBM
C  T IS IN DEG RANKINE
C
      FUNCTION HG(T)
      A=42.14702865
      B=-4344.343807
      C=-12.84596753
      D=.004008372507
      E=.0313605356
      F=862.07
      R=.078117
      BB=.0019
      A2=-3.126759
      B2=.001318523
      C2=-35.76999
```

```
      A3=-.025341
      B3=4.8721215-5
      C3=1.220367
      A4=.0016887277
      B4=-3.6070625E-6
      A5=-2.35893E-5
      B5=2.4423C3E-8
      C5=-1.47E379E-4
      A6=1.0575042E8
      B6=-9.472103E4
      TC=848.07
      AK=-4.5
      A1=.023815
      B1=-336.80703
      C1=2.798923E-4
      D1=-2.123734E-7
      E1=8.999018E-11
      TO=-40.+459.67
      PTBO=PSAT(TO)*ALOG(10.)*(-B/TO/TO+C/TO/ALOG(10.)+D-
     *E*F/TO/TO*ALOG10(F-TO)-E/TO/ALOG(10.))
      V2=VG(TO)
      V1=VF(TO)
      H2=PTBO*TO*(V2-V1)*.185053
      U2=H2-PSAT(TO)*V2*.185053
      GT=AK/TC*T
      GTO=AK/TC*TO
      VB=V2-9R
      VT=VG(T)
      VTB=VG(T)-9R
      U32=(C2/VB+.5*C3/VB/VB+.25*C5/VB**4.)*
     *(EXP(GT)*(GT-1.)-EXP(GTO)*(GTO-1.))*.185053-
     *A1*(T-TO)+B1*(1./T-1./TO)-.5*C1*(T*T-TO*TO)-
     *D1/3.*(T**3.-TO**3.)-.25*E1*(T**4.-TO**4.)
      U63=(-A2+C2*(GT-1.)*EXP(GT))*(1./VTB-1./VB)+
     *(-A3+U3*(GT-1.)*EXP(GT))*.5*(1./VTB**2.-1./VB**2.)-
     *A4*1./3.*(1./VTB**3.-1./VB**3.)+
     *(-A5+C5*(GT-1.)*EXP(GT))*.25*(1./VTB**4.-1./VB**4.)
      U6=-U32-U63*.185053+U2
      H6=U6+PSAT(T)*VT*.185053
      RETURN
      END
C
C
C  FUNCTION HF CALCULATES ENTHALPY OF SATURATED LIQUID FREON-11
C  HF IS IN BTU/LBM
C  T IS IN DEG RANKINE
C
      FUNCTION HF(T)
      B=-4344.343807
      C=-12.84596753
      D=.004008372507
      E=.0313605356
```

```
      F=862.07
      PTS=PSAT(T)*ALOG(10.)*(-B/T/T+C/T/ALOG(10.)+D-
     *E*F/T/T*ALOG10(F-T)-E/T/ALOG(10.))
      HFG=PTS*T*(VG(T)-VF(T))*.185053
      HF=HG(T)-HFG
      RETURN
      END
C
C
C  FUNCTION SG CALCULATES ENTROPY OF SATURATED VAPOR FREON-11
C  SG IS IN BTU/LBM DEG RANKINE
C  T IS IN DEG RANKINE
C
      FUNCTION SG(T)
      A=42.14702865
      B=-4344.343807
      C=-12.84596753
      D=.004008372507
      E=.03136053356
      F=862.07
      R=.078117
      BB=.0019
      A2=-3.126759
      B2=.001318523
      C2=-35.76999
      A3=-.025341
      B3=4.875121E-5
      C3=1.220367
      A4=.001687277
      B4=-1.805062E-6
      A5=-2.35893E-5
      B5=2.448303E-8
      C5=-1.478379E-4
      A6=1.057504E8
      B6=-9.472103E4
      TC=388.07
      AK=-4.5
      A1=.023815
      B1=-336.80703
      C1=2.798823E-4
      D1=-2.123734E-7
      E1=5.999018E-11
      TO=-40.+459.67
      PTSO=PSAT(TO)*ALOG(10.)*(-B/TO/TO+C/TO/ALOG(10.)+D-
     *E*F/TO/TO*ALOG10(F-TO)-E/TO/ALOG(10.))
      V2=VG(TO)
      V1=VF(TO)
      H2=PTSO*TO*(V2-V1)*.185053
      S2=H2/TO
      G=AK/TC
      GT=G*T
      GTO=G*TO
```

```
      VB=V2-BB
      VT=VG(T)
      VTB=VG(T)-BB
      S32=G*(C2/VB+.5*C3/VB/VB+.25*C5/VB**4.)*
     *(EXP(GT)-EXP(GTO))*.185053-
     *A1*(ALOG(T)-ALOG(TO))+.5*B1*(1./T/T-1./TO/TO)-C1*(T-TO)-
     *D1/2.*(T**2-TO*TO)-E1/3.*(T**3.-TO**3.)
      S63=R*(ALOG(VB)-ALOG(VTB))+(B2+C2*G*EXP(GT))*(1./VTB-1./VB)+
     *(C3+C3*G*EXP(GT))*.5*(1./VTB/VTB-1./VB/VB)+
     *B4/3.*(1./VTB**3.-1./VB**3.)+
     *(B5+C5*G*EXP(GT))*.25*(1./VTB**4.-1./VB**4.)
      S6=-S32-S63*.185053+S2
      RETURN
      END
C
C
C  FUNCTION SF CALCULATES ENTROPY OF SATURATED LIQUID FREON-11
C  SF  IS IN BTU/LBM DEG RANKINE
C  T  IS IN DEG RANKINE
C
      FUNCTION SF(T)
      B=-4344.343807
      C=-12.84596753
      D=.004008372507
      E=.03136605356
      F=848.07
      PTS6=PSAT(T)*ALOG(10.)*(-B/T/T+C/T/ALOG(10.)+D-
     *E*F/T/T*ALOG10(F-T)-E/T/ALOG(10.))
      SFG=PTS6*(VG(T)-VF(T))*.185053
      SF=SG(T)-SFG
      RETURN
      END
C
C
C  FUNCTION CV CALCULATES HEAT CAPACITY OF VAPOR FREON-11 AT CONSTANT
C  VOLUME
C  CV  IS IN BTU/LBM DEG F
C  T  IS IN DEG RANKINE
C
      FUNCTION CV(T)
      BB=.0019
      C2=-35.76999
      C3=1.220367
      C5=-1.478379E-4
      AK=-4.5
      A1=.023815
      B1=-336.80703
      C1=2.798823E-4
      D1=-2.123734E-7
      E1=5.999018E-11
      TC=848.07
      GK=AK/TC
```

```
      GT=GK*T
      VT=VG(T)-BB
      CV=(-C2/VT-C3/VT/VT-C5/VT**4.)*
     *(EXP(GT)*GK*GK*T)*.185053+A1+B1/T/T+C1*T+
     *D1*T*T+E1*T**3.
      RETURN
      END
C
C
C  FUNCTION CP CALCULATES HEAT CAPACITY OF VAPOR FREON-11 AT CONSTANT
C  PRESSURE
C  CP IS IN BTU/LBM DEG F
C  T IS IN DEG RANKINE
C
      FUNCTION CP(T)
      DT=1.
      T3=T+DT
      P=PSAT(T)
      V0=VG(T)
      V1=VG(T-5.)
      TOL=V0*1E-5
    2 V2=V0+(V1-V0)/2.
      IF((V1-V0)/2.LT.TOL) GO TO 1
      IF(FCPV3(P,T3,V0)*FCPV3(P,T3,V2).GT.0.)THEN
      V0=V2
      ELSE
      V1=V2
      ENDIF
      GO TO 2
    1 V3=V2
      TA=T-5.
      TB=T
      TOL=1.E-4
    3 TP=TA+(TB-TA)/2.
      IF((TB-TA)/2.LT.TOL) GO TO 4
      IF((VG(TA)-V3)*(VG(TP)-V3).GT.0.)THEN
      TA=TP
      ELSE
      TB=TP
      ENDIF
      GO TO 3
    4 TS=TP
      BB=.0019
      C2=-38.76999
      C3=1.220367
      C5=-1.478379E-4
      A1=.023815
      C1=2.798823E-4
      D1=-2.123734E-7
      E1=5.999018E-11
      TC=848.07
      AK=-4.5
```

```
      VB=VR(TS)-BB
      GT=AK/TC*T3
      GTO=AK/TC*TS
      U23=(C2/VB+.5*C3/V3/VB+.25*C5/V3**4.)*
     *(EXP(GT)*(GT-1.)-EXP(GTO)*(GTO-1.))*.185053-
     *A1*(T3-TS)+B1*(1./T3-1./TS)-.5*C1*(T3*T3-TS*TS)-
     *D1/3.*(T3**3.-TS**3.)-.25*E1*(T3**4.-TS**4.)
      HG2=-U23+(P-PSAT(TS))*V3*.185053
      CP=(HG2+HG(TS)-HG(T))/DT
      RETURN
      END


C
C     FUNCTION FCPV3 WILL BE USED IN FUNCTION CP TO EVALUATE
C   CP FROM THE RELATIONSHIP BETWEEN CP AND CV
C
      FUNCTION FCPV3(P,T,V)
      R=.079117
      RB=.0019
      A2=-3.126759
      B2=.001318523
      C2=-35.76999
      A3=-.025341
      B3=1.875121E-5
      C3=1.220367
      A4=.001627277
      B4=-1.205062E-6
      A5=-2.35893E-5
      B5=2.448203E-8
      C5=-1.473379E-4
      A6=1.057504E8
      B6=-4.472103E4
      TC=848.07
      AK=-4.5
      PP=EXP(AK*T/TC)
      VB=V-BB
      FCPV3=R*T/VB+(A2+B2*T+C2*PP)/VB/VB+(A3+B3*T+C3*PP)/VB**3.+
     *(A4+B4*T)/VB**4.+(A5+B5*T+C5*PP)/VB**5.-P
      IF(V.GT..1)GO TO 1
      FCPV3=FCPV3+(A6+B6*T)/EXP(580.*V)
    1 RETURN
      END
```